NASA/TP—2010–216437

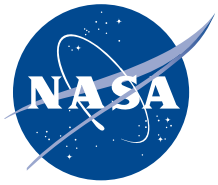

Documentation of Stainless Steel Lithium Circuit Test Section Design

T.J. Godfroy
Maximum Technology Corporation, Huntsville, Alabama

J.J. Martin
Marshall Space Flight Center, Marshall Space Flight Center, Alabama

With Supplemental Information by

E.T. Stewart
Marshall Space Flight Center, Marshall Space Flight Center, Alabama

N.O. Rhys
Yetispace, Inc., Huntsville, Alabama

August 2010

The NASA STI Program…in Profile

Since its founding, NASA has been dedicated to the advancement of aeronautics and space science. The NASA Scientific and Technical Information (STI) Program Office plays a key part in helping NASA maintain this important role.

The NASA STI Program Office is operated by Langley Research Center, the lead center for NASA's scientific and technical information. The NASA STI Program Office provides access to the NASA STI Database, the largest collection of aeronautical and space science STI in the world. The Program Office is also NASA's institutional mechanism for disseminating the results of its research and development activities. These results are published by NASA in the NASA STI Report Series, which includes the following report types:

- TECHNICAL PUBLICATION. Reports of completed research or a major significant phase of research that present the results of NASA programs and include extensive data or theoretical analysis. Includes compilations of significant scientific and technical data and information deemed to be of continuing reference value. NASA's counterpart of peer-reviewed formal professional papers but has less stringent limitations on manuscript length and extent of graphic presentations.

- TECHNICAL MEMORANDUM. Scientific and technical findings that are preliminary or of specialized interest, e.g., quick release reports, working papers, and bibliographies that contain minimal annotation. Does not contain extensive analysis.

- CONTRACTOR REPORT. Scientific and technical findings by NASA-sponsored contractors and grantees.

- CONFERENCE PUBLICATION. Collected papers from scientific and technical conferences, symposia, seminars, or other meetings sponsored or cosponsored by NASA.

- SPECIAL PUBLICATION. Scientific, technical, or historical information from NASA programs, projects, and mission, often concerned with subjects having substantial public interest.

- TECHNICAL TRANSLATION. English-language translations of foreign scientific and technical material pertinent to NASA's mission.

Specialized services that complement the STI Program Office's diverse offerings include creating custom thesauri, building customized databases, organizing and publishing research results…even providing videos.

For more information about the NASA STI Program Office, see the following:

- Access the NASA STI program home page at <http://www.sti.nasa.gov>

- E-mail your question via the Internet to <help@sti.nasa.gov>

- Fax your question to the NASA STI Help Desk at 443–757–5803

- Phone the NASA STI Help Desk at 443–757–5802

- Write to:
  NASA STI Help Desk
  NASA Center for AeroSpace Information
  7115 Standard Drive
  Hanover, MD 21076–1320

NASA/TP—2010–216437

Documentation of Stainless Steel Lithium Circuit Test Section Design

T.J. Godfroy
Maximum Technology Corporation, Huntsville, Alabama

J.J. Martin
Marshall Space Flight Center, Marshall Space Flight Center, Alabama

With Supplemental Information by

E.T. Stewart
Marshall Space Flight Center, Marshall Space Flight Center, Alabama

N.O. Rhys
Yetispace, Inc., Huntsville, Alabama

National Aeronautics and
Space Administration

Marshall Space Flight Center • MSFC, Alabama 35812

August 2010

Acknowledgments

Many thanks to the following for the long hours and excellent work on this project: Roger Harper, Dr. Noah O. Rhys, Alok Majumdar, Stan McDonald, Gene Fant, Kenny Webster, Melissa Van Dyke, and Eric Stewart.

TRADEMARKS

Available from:

NASA Center for AeroSpace Information
7115 Standard Drive
Hanover, MD 21076–1320
443–757–5802

This report is also available in electronic form at
<https://www2.sti.nasa.gov>

TABLE OF CONTENTS

TABLE OF CONTENTS (Continued)

LIST OF FIGURES

LIST OF FIGURES (Continued)

LIST OF FIGURES (Continued)

LIST OF TABLES

LIST OF ACRONYMS, SYMBOLS, AND ABBREVIATIONS

Ar	argon
ATM	atmosphere
B_4C	boron carbide
Be	beryllium
BHTC	bottom heater thermocouple
C	carbon
CAD	computer-aided design
Cr	chromium
Cu	copper
EFF–TF	Early Flight Fission–Test Facility
EM	electromagnetic
GFSSP	generalized fluid system simulator program
GHe	gaseous helium
GN_2	gaseous nitrogen
H_2	hydrogen
He	helium
HOV	hand-operated valve
HX	heat exchanger
Li	lithium
LR	lower reservoir

LIST OF ACRONYMS, SYMBOLS, AND ABBREVIATIONS (Continued)

LRHA	lower reservoir thermocouple
LRHB	lower reservoir thermocouple
LRHC	lower reservoir thermocouple
LRPG	lower reservoir pressure gauge
LRTC	lower reservoir thermocouple
MLI	multilayer insulation
MSFC	Marshall Space Flight Center
N_2	nitrogen
Na	sodium
NaK	sodium-potassium
Ni	nickel
NRPCT	Naval Reactors Prime Contract Team
O_2	oxygen
ROV	remote operated valve
SCCM	standard cubic centimeters per minute
Si	silicon
SS	stainless steel
T	tube
TC	thermocouple
THTC	top heater thermocouple
TP	Technical Publication

UO_2	uranium oxide
UR	upper reservoir
VCR	vacuum coupling radiation

NOMENCLATURE

C_p	specific heat
$\dot{m}$	mass flow
p	pressure
Q	energy (input heat)
T	temperature
ΔP	change in pressure
ΔT	change in temperature

TECHNICAL PUBLICATION

DOCUMENTATION OF STAINLESS STEEL LITHIUM CIRCUIT TEST SECTION DESIGN

1. INTRODUCTION

The Early Flight Fission–Test Facility (EFF–TF) was established by the Marshall Space Flight Center (MSFC) Propulsion Research Center Nuclear Propulsion Group to perform hardware-directed activities relevant to multiple nuclear power reactor concepts using nonnuclear test methodology. This includes fabrication and testing at the module/component level and near-prototypic hardware configuration allowing for realistic thermal hydraulic evaluations of systems. In addition, equally important to the actual hardware development are: (1) the experience and knowledge gained during fabrication and assembly, (2) the development of documentation and procedures related to integration and operation (includes both test hardware and facilities), and (3) the experience gained from early hardware testing with relevant materials and environment producing insight and lessons learned for the hardware development program. There are a number of reactor and primary heat transport systems applicable to space-based power and propulsion. The EFF–TF examined a pumped alkali metal lithium (Li) circuit for the Naval Reactors Prime Contract Team (NRPCT). During development of this system, required facility interfaces were leveraged off of existing EFF–TF capabilities and test hardware wherever possible. In addition, baseline documentation (including procedures, safety, hazards, etc.) evolved to augment the current EFF–TF operations.

The intent of this work was to gain experience with a Li liquid metal system and to begin to understand the nature of liquid Li, freeze/thaw issues, and operational issues. Specific objectives included:

- Design, fabricate, assemble, and operate a small-scale stainless steel (SS) actively pumped liquid metal (Li) flow circuit.
- Gain circuit experience with Li such that the experience can be transferred, where applicable, to follow-on design and testing of a high-temperature, refractory metal actively pumped Li circuit.
- Investigate the nature of freeze/thaw issues through hardware testing.
- Include, by design, the ability to perform component testing of nominally-sized components that may be of interest to NRPCT.
- Document lessons learned for future applications.

2. DESIGN CHANGE TO LITHIUM

The Li design for an actively pumped circuit was based on an existing actively pumped sodium-potassium (NaK) design.

To establish an active circuit in a short amount of time, NRPCT utilized the existing NaK core, heat exchanger (HX), and pump. These components were designed and fabricated or procured for a NaK system but would suffice for a Li system with no modifications. However, due to the change to Li, the issues of Li and SS incompatibility, the higher melting point of Li, and the unknown wetting temperature had to be evaluated.

2.1 Lithium General Description

Lithium is silvery in appearance. It is a solid about half as dense as water at room temperature. The melting point is 180.5 °C (356.9 °F) and it has the highest specific heat of any solid element, making it well suited for some heat transfer applications. The material texture is very sticky or tacky. A 1-in-diameter bar is more easily cut with pruning shears than a hack saw. A reasonable description of the strength of solid Li is that it has the consistency of a 'Tootsie Roll that has been refrigerated.'[1] It must be handled in an inert environment, such as argon (Ar), as it has a great affinity for (but not limited to) nitrogen (N_2) and oxygen (O_2) and will immediately tarnish in open air. Care must be taken when storing Li, and proper personal protection should be worn at all times. It is corrosive, especially at elevated temperatures (e.g., at circuit operating temperature), and special care must be taken to avoid injury to personnel. A brief review of Li thermophysical properties can be found in reference 1.

2.2 Stainless Steel and Lithium Incompatibility

There are several mechanisms that work to corrode the SS in an actively pumped Li circuit. For austenitic steels, the initial stage of high dissolution rates corresponds to the formation of a ferrite layer that results from the preferential leaching of nickel (Ni) and, to a lesser extent, chromium (Cr) from the surface of the steel.[2] These constituents are then observed to deposit downstream in lower temperature regions, preferentially coming out of solution based on temperature. As might be expected, the mass transfer of the system also demonstrates a significant temperature dependence, and as such, the overall changes in temperature (ΔT) of the system must be considered.[3] Additionally, high N_2 levels in the Li circuit lead to general dissolution in austenitic steels and a 'stoichiometric' steady-state dissolution behavior may not be achievable in a flowing Li environment.

For this circuit, the primary concern associated with these corrosion mechanisms is failure of the SS boundary. The rate of corrosion is estimated to be ≈22 μm/yr at 427 °C (800.6 °F) and is slightly lower at 482 °C (899.6 °F).[2] This rate was used to estimate the system operating time to reach failure even though the circuit was anticipated to operate at a slightly higher temperature, ≈500 °C (932 °F). Extensive literature searches revealed that the corrosion mechanisms for Li are not as well characterized as for other alkali metals, such as sodium (Na), requiring an approximation of this nature. The highest temperature

region will be in the core, where the inner tube has a thickness of 0.089 cm (0.035 in). The potential SS corrosion rate in this region would result in failure after ≈40.5 yr of operation; potential failure due to pressure was not considered in this calculation. Considering the anticipated operational lifespan of this circuit of ≈1,000 hr and low-pressure operation of ≈103.4 kPa (≈15 psia), this rate of corrosion was considered acceptable and posed minimal risk. However, steps were still taken to minimize the ΔT in the system as well as to limit the introduction of N_2 into the system. This was accomplished by purchasing high-purity Li, using Ar cover gas where appropriate, and operating the circuit in a vacuum. There was no planned active measurement of the N_2 levels in the Li circuit; however, samples of Li were taken initially and periodically during testing, if possible, in an attempt to quantify the level of contamination. By design, the impurity levels in this circuit were not to be of primary concern. For a more detailed discussion on corrosion mechanisms, see reference 2.

2.3 Lithium Melting Temperature

The melting point of Li is 180.5 °C (356.9 °F). As such, the circuit must be preheated to allow introduction of Li to the system. However, because the freeze/thaw behavior in this type of configuration is undetermined, it is necessary to drain the system before it is allowed to cool. It should be noted that, because Li contracts as it freezes, this process is not the concern; however, as the Li thaws, a condition may arise where the expansion of the melted Li exceeds the yield strength of the SS due to unknown/unpredictable void formation during freeze. Additionally, in the event of power loss, the system must be drained quickly before it cools and freezes, thereby resulting in unknown conditions upon thaw. For these reasons, the fill/drain reservoir was relocated to the lowest vertical position, and an expansion reservoir was added to accommodate the ≈4.5% thermal expansion of the Li at operational temperatures.

2.4 Wetting

Wetting is a concern for any liquid metal. Wetting provides maximum thermal transfer from the boundary metal, SS in this application, to the liquid metal. Wetting is a function of temperature and the impurity concentrations in the liquid metal and on the boundary metal surface. To achieve wetting, the liquid metal must bring into solution the impurities that are present on the surface of the metal to be wet; as the type and quantity of impurities increase so does the temperature required to drive them into solution. The most cost-effective, time-efficient method to evaluate the temperature at which wetting would occur for this circuit was to measure it directly. Relatively impure Li, 98%, in a cleaned but unbaked SS beaker was heated over ≈45 min to ≈340 °C (644 °F) in an Ar environment with <0.3 ppm O_2 and <1 ppm water vapor. The observed wetting temperature was ≈310 °C (590 °F). This was noted by the angle of incidence of the Li droplet as it transitioned from acute to obtuse. From this experiment, it was concluded that, with higher purity Li and a fully baked-out system, wetting will occur below this temperature. Once the entire circuit is brought to ≈325 °C (617 °F), it can be assumed to have properly wet all surfaces. The exception to this will be in the standoff regions that lead to the pressure transducers because they are maintained at a lower temperature; however, this will not affect the performance of the pressure transducers and a lack of wetting may actually be preferred in this area.

3. LIQUID METAL CORE DESIGN BASIS

The liquid metal circuit was designed around the core design. While this core design was based on a NaK design study, the application of this design to a working Li design still has significant merit. The core geometry for this project, based on a 100-kW study performed by the Los Alamos National Laboratory, utilizes annular fuel pins and two-pass coolant flow.[4] Section 3.1 details the design with NaK as the reactor coolant.

3.1 Core Design—A Los Alamos National Laboratory Design Study

Figure 1 illustrates the general layout of the core assembly with NaK coolant loops and plenums. The coolant enters the core through an annular inlet plenum (positioned at the top) that directs the coolant into a circumferential flow passage formed between the outer shell and core block. The flow follows this perimeter passage, traversing the length of the core and exiting into the lower manifold. This manifold distributes the coolant for a return trip to the top of the core via annular gaps formed between the fuel pin clad and core block. At the top of the core, an outlet plenum collects the heated NaK. Figure 2 shows an end view of this same core design layout, illustrating both the perimeter and annular fuel pin flow paths. Design study specifics include the following dimensional parameters:

- Twelve-sided SS core block:
  - Outer diameter = 25.75 cm (10.14 in), point to point.
  - Length = 68 cm (26.8 in).

- Fuel pin holes (in core block):
  - Number = 127.
  - Diameter = 1.73 cm (0.680 in).
  - Length = through core block.
  - Hole pitch = 1.90 cm (0.75 in), center to center of hole.
  - Web = 0.18 cm (0.070 in), core block material between holes.

- Fuel pins (clad):
  - Outer diameter = 1.4 cm (0.55 in with 0.035-in wall).
  - Length = 74 cm (29.13 in), length to clear outer pressure shell.
  - Radial gap to core = 0.0064 cm (0.0025 in).

- Outer pressure shell:
  - Outer diameter = 26.4 cm (10.4 in with 0.10-in wall).
  - Length = 78 cm (30.7 in), sufficient to form upper/lower plenums.

- Thermal simulators (heaters):
  - Outer diameter = 1.15 cm (0.453 in leaves a 0.013-in gap).
  - Heated length = 60 cm (23.62 in).

- Coolant specifics:
  – Inlet temperature = 615 °C (1,139 °F).
  – Exit temperature = 650 °C (1,202 °F).
  – Flow rate = 3.25 kg/s (68.7 g/min).
  – Core net ΔP = 6.9 kPa (1.04 psi).

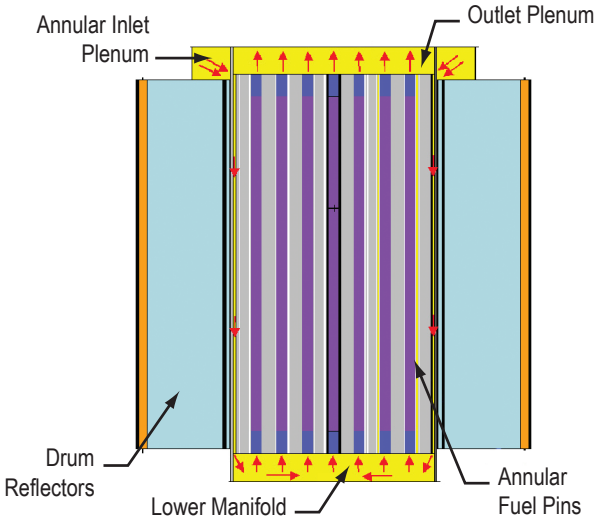

Figure 1. General core NaK flow loop.

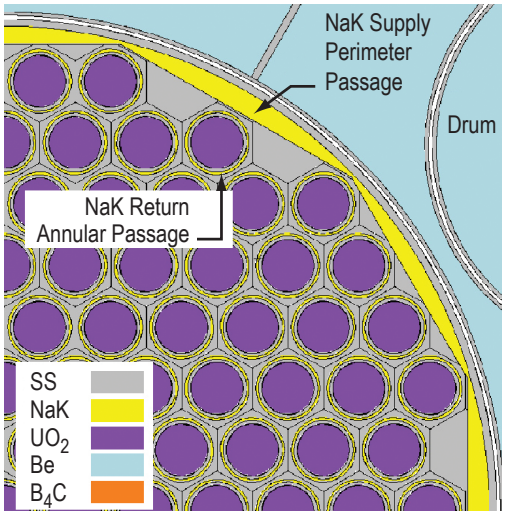

Figure 2. Core end view showing flow passages.

For the sake of simplifying hardware fabrication, integration, and testing while staying within overall project funding, the selected approach requires that:

- Both the reflector drums and shields located beyond the outer pressure shell are eliminated from the test hardware layout.

- A one-third-power version of the core assembly is employed. This requires that a subset or partial array of the core geometry be used; specifically, the geometry encompasses the central three fuel pin rings (total of 37 pins), shown in figure 3. All geometric dimensions for the fuel pins and flow passages are maintained.

- All other system components are designed as facility elements using standard design practices that err on the side of reliable, producing heavier rather than 'flight like' components.

The reduction of core size for the purposes of an initial test has a significant impact on overall complexity and cost. The reduction in power level eliminates the requirement for two pumps (off-the-shelf style 6 units) and flow balancing issues, reduces the size of HXs/flow plumbing, and significantly decreases the required number of thermal simulators (heaters).

Target core design goals for the reduced 37-pin system include the following specifics:

- Total fuel pins = 37.
- Input power = 30 kW.
- Coolant flow rate = 1 kg/s (2.21 lb/s).
- Core pressure drop = 6.8 kPa (0.986 psi).
- Inlet temperature = 615 °C (1,139 °F).
- Outlet temperature = 650 °C (1,202 °F).

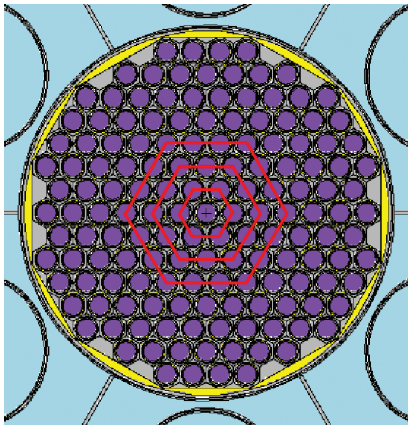

Figure 3. End view of core showing inner three fuel pin rings for test hardware fabrication.

4. STAINLESS STEEL LITHIUM CIRCUIT LAYOUT

A general flow diagram, illustrated in figure 4, identifies the key system elements of the SS Li flow circuit. The complete system is mounted on a tilt table (making it modular) that is inserted into the EFF–TF 9-ft vacuum chamber located in Building 4655. The interfaces/connections with the vacuum chamber include instrumentation, pump/heater power, pump cooling, valve control power, and a secondary helium (He) Ar closed-cycle coolant loop (no Li is routed out of the vacuum chamber). The Li circuit is an all-welded construction with the exception of a few strategic locations to attach instrumentation such as the liquid level sensors, pressure transducers, and test section connection/disconnection points. These connections are all made with VCR® (a Swagelok Co. product) fittings. All components and tubing have been proof pressure tested to 2,068 kPa (>300 psi) and leak checked using gaseous helium (GHe) to better than 10^{-9} standard cm^3 per minute (SCCM) to minimize the potential for leaks. High-temperature valves (remote operated where needed) are used at the lower reservoir. Instrumentation measurements are made at key locations including the core, HX, reservoir, and pump as well as at necessary points throughout the circuit. All components are constructed from SS, primarily 316, with the exception of the level sensors. The ceramic portions of the sensors do not come in direct contact with the Li.

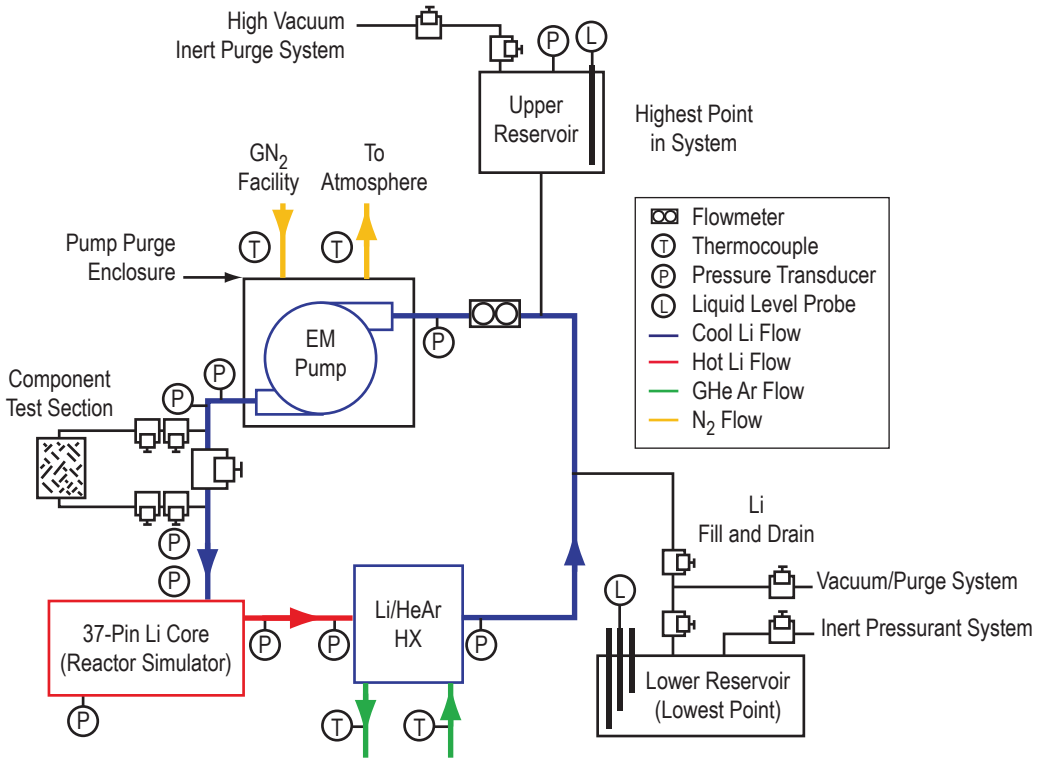

Figure 4. Simplified schematic for SS Li thermal hydraulic flow circuit.

Based on this schematic, a detailed engineering design evolved, resulting in the overall system drawing set included in sections A–H in the supplemental information. The final hardware configuration based on these drawings is illustrated in the three-dimensional rendering presented in figure 5. Figure 6 shows the as-built test circuit. The overall layout of components and tubing was configured to provide sufficient flexibility without the use of expansion bellows in the circuit. Bellows were avoided because (1) they are a thin-walled component susceptible to mechanical damage, and (2) the convolutes can retain residual Li making draining/cleanup more difficult. Additionally, butt welds were used wherever possible to eliminate possible cavities in which Li and impurities could be trapped. The flow circuit was designed for use on a tilt table, providing a 'low spot' in order to utilize gravity to route the Li to the fill/drain vessel (lower reservoir). In the smaller diameter tube sections, such as in the pressure transducer standoffs, a purge of high purity Ar was envisioned to overcome the surface tension of the Li and to purge the lines of the liquid Li. In general, major flow components are laid out to limit pressure drop (large flow areas) so as to maximize flow rate and to minimize pump power consumption. The sections that follow will describe the major system components in more detail.

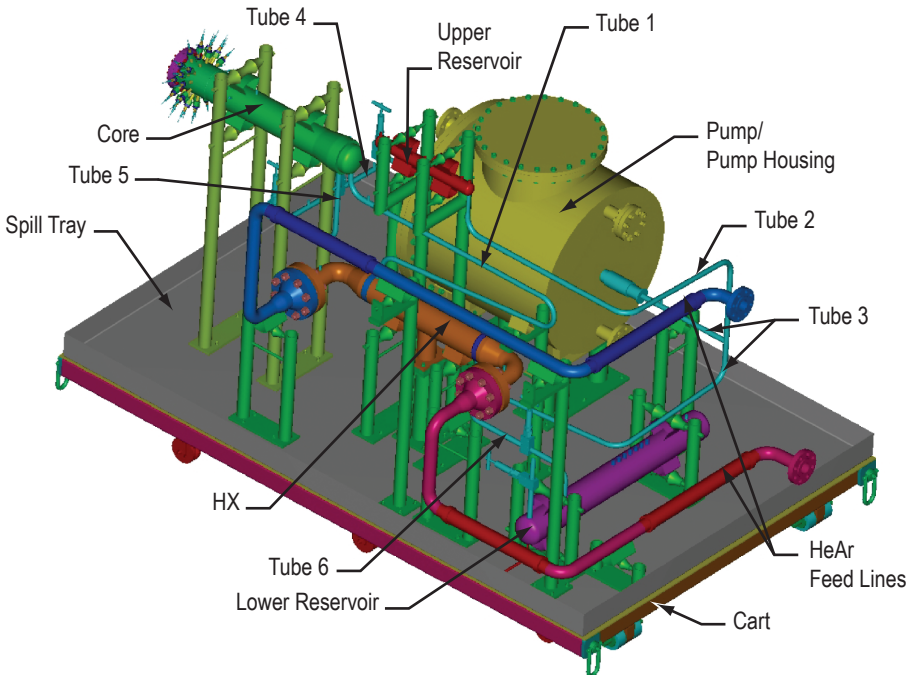

Figure 5. Lithium test circuit as designed.

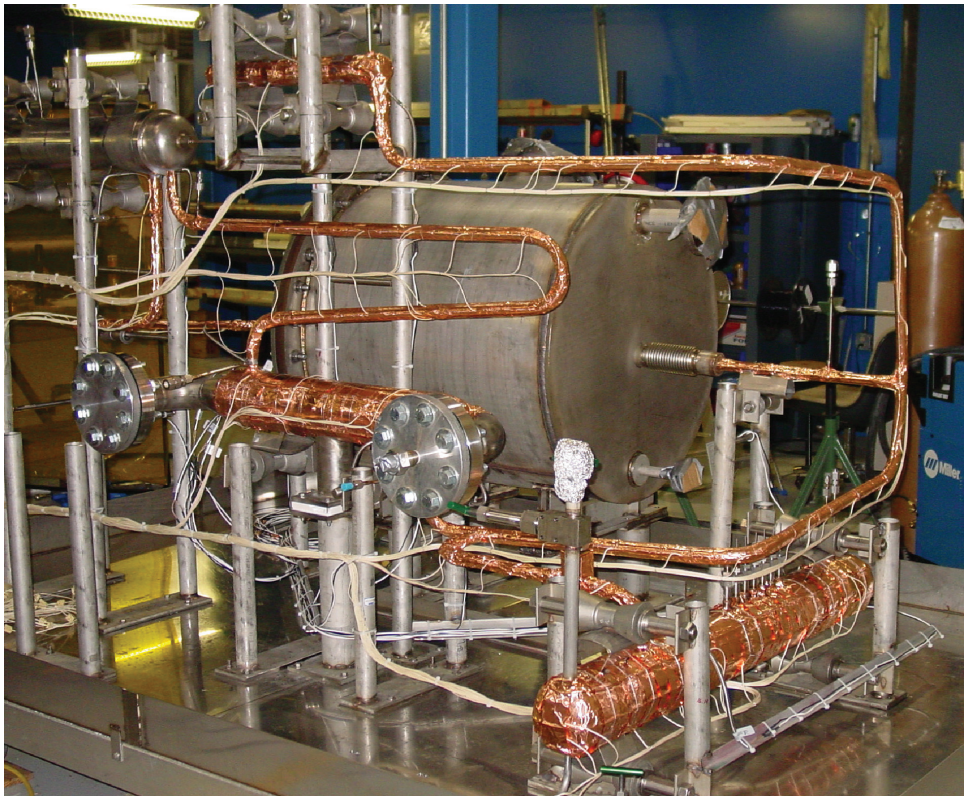

Figure 6. Lithium test loop as built (HeAr feed lines not shown).

The volume of each major component and the overall plumbing are listed in table 1. The total system volume is estimated at 7.51 kg (16.56 lb), based on computer-aided design (CAD) models of the as-built circuit. Lithium is loaded at ≈250 °C (≈482 °F); at 500 °C (900 °F), the Li in the circuit will expand to fill 7.51 kg (16.56 lb) of volume. The tubing leading to the upper reservoir was sized to accommodate the volume expansion of the Li; this was necessary to provide sufficient margin for fluid expansion when brought from the load temperature to the operating temperature of 500 °C (900 °F). The lower reservoir was designed to be of sufficient volume to contain all the Li at the maximum operational temperature, 500 °C (900 °F) (the maximum Li volume).

Table 1. System volume breakdown (estimated by CAD models of engineering drawings).

	Volume		Lithium Mass at 500 °C (900 °F)	
Component	**(cm^3)**	**(in^3)**	**(kg)**	**(lb)**
Core assembly	5,424	331	2.61	5.75
HX	5,440	332	2.61	5.75
Tubing/pump	3,736	228	1.79	3.95
Upper reservoir	1,049	64	0.5	1.10
Total	**15,649**	**955**	**7.51**	**16.56**
Lower reservoir	16,928	1,033	8.13	17.92

4.1 Lithium

A list of the predominant suppliers of high-purity Li in the United States is found in reference 5. Companies having the capability to provide Li of sufficient purity for the operations planned at the EFF–TF and with the capability of providing the larger quantities necessary for the ultimate circulating loop (assume ≈15 kg (≈33.07 lb)) are identified. Certain nonmetallic impurities can significantly affect the structural integrity of containment materials in Li operations; specifically N_2, O_2, carbon (C), silicon (Si), and hydrogen (H_2) are of interest in this application. It was assumed that the desired purity level was <100 ppm of any single nonmetallic impurity, as this purity level matches that of the Li in the cited corrosion references.

Lithium is generally shipped using one of two transport methods, either of which is designed to prevent contact of the Li metal with the atmosphere. The sample may be packed in a vacuum can with a mineral oil coating over the stock material, or it may be packed in a vacuum can with Ar used as a cover gas. To maintain the integrity of the Li purity from manufacture to receipt at the EFF–TF, all procured material was vacuum packed with an Ar cover gas. Per discussions with product managers from various companies, the maximum purity Li currently available commercially is 99.97%. Given the available purity levels and ease of working with the vendor, the top two choices for Li vendors were American Elements Corp. and ESPI Metals. All Li for this task was purchased from ESPI.

4.2 Instrumentation

4.2.1 Temperature

All circuit temperature measurements are performed using type-K thermocouples (TCs) that are spot welded directly to the SS. The TC wire, manufactured by Omega (HH–K–24–SLE), is a high temperature, glass-jacketed, 24-gauge wire capable of operation at up to 704 °C (1,299 °F). There is one thermowell located at the exit plenum of the core. The TCs are located approximately every 15.24 cm (6 in) along the lengths of tubing and in distributed patterns over the remaining components. These diagnostics monitor circuit temperature distribution and help provide system diagnosis. Additional TCs are placed on system components to provide backup to other instrumentation systems, such as level measurement or trace heater operational temperature. The TCs are all terminated with miniconnectors that plug into a distribution panel inside the vacuum chamber. A feedthrough carries the signal out of the chamber to IOTech® data acquisition hardware. This signal is then converted to a temperature measurement in degrees Celsius and read into a custom LabVIEW™ (a National Instruments® product) interface where it is recorded to file.

4.2.2 Pressure

The pressure transducers selected for this circuit were manufactured by Astro Sensors, model number AS9001–SP. Cryogenic units were modified to a pressure range of zero to 172.4 kPa (zero to 25 psia), an output signal of zero to 30 mV at 3 mV/V, and a compensated range from 20 to 218 °C (68 to 424.4 °F). The static accuracy for this unit is 0.1% of full scale, all wetted parts are 316 SS, the diaphragm thickness is >0.013 cm (0.005 in), and it has a flowthrough design. The flowthrough design provides a method for an inert gas purge that is used to push the liquid Li out of the transducer pressure sense

area. A vacuum coupling radiation- (VCR-) type connection is used to couple the pressure transducers to the system.

TCs were placed along the length of the transducer standoff. A calculation was performed to determine the required standoff length to keep the transducer cool enough to operate reliably (sec. I in the supplemental information). The results of this study show that if the main flow path has an operating temperature of 600 °C (1,112 °F), a standoff of ≈25 cm (≈9.84 in) will be required to allow the Li to cool below freezing. An additional 10 cm (3.94 in) were added to this length and a heater was applied in the region just before the transducer. This additional length is calculated to be sufficient to allow the Li temperature to drop down into the operational range of the pressure transducer. If the Li temperature becomes too low, additional heat can be added by this heater. If problems do arise with the transducer, the VCR connection will allow for rapid replacement or capping of the standoff. The signal from the transducer is routed to a feedthrough on the chamber and then to a National Instruments SCXI chassis where it is converted to a pressure measurement.

4.2.3 Level

Level measurement was needed on the upper reservoir and on the lower reservoir. Figure 7 shows a 5-kV, 30-A power feedthrough that is sold by Kurt Lesker Company. The level sensors are high voltage, high current electrical feedthroughs terminating in weld lips that are welded to a VCR fitting. This is then mated to a VCR fitting on the upper and lower reservoirs. The level sensor works by completing a circuit when the level of the Li comes in contact with the SS pin of the feedthrough.

Figure 7. Level sensor.

4.2.4 Flow

Flow measurement is measured in two ways. The first method uses the HX to estimate flow from the relationship,

$$Q = \dot{m} C_p \Delta T \ , \tag{1}$$

where, in a reasonably well insulated HX, the energy coming in will be equal to that removed:

$$Q_{\mathrm{Li}} = Q_{\mathrm{He}} \ . \tag{2}$$

The inlet and outlet temperatures of the gas and the gas flow rate are measured, and the specific heat (C_p) is known for the gas. Therefore, the Li mass flow rate can be calculated from equation (3):

$$\dot{m}_{\mathrm{Li}} = \frac{\dot{m}_{\mathrm{He}} C_{p,\mathrm{He}} \Delta T_{\mathrm{He}}}{C_{p,\mathrm{Li}} \Delta T_{\mathrm{Li}}} \quad . \tag{3}$$

Lithium flow measurement can also be accomplished using a permanent magnet. The magnet is used to measure the current induced in a wire, which then can be correlated to the Li flow rate. The most difficult part of any flow measurement is the calibration of the device. It is hoped that these two methods corroborate each other.

4.3 Trace Heating and Insulation

4.3.1 Trace Heaters

Trace heaters are placed on nearly all circuit components and tubing such that the entire system can be heated to ≈525 °C (≈977 °F). The trace heaters used are Watlow brand cable heaters that are SS sheathed, 0.318-cm- (0.125-in-) diameter cold formable, 240-V ac resistance heaters capable of continuous operation at temperatures up to 650 °C (1,202 °F) and with intermittent operating periods up to 815 °C (1,499 °F). These heaters were cold formed to fit as snuggly as possible along all sections of tubing and all major components except the core. An attempt was made to provide two trace heaters for each heated section and to make logical sections for control of thermal input into the system.

The first use of the trace heaters was in the conditioning phase to outgas the tubing and other components by performing high-temperature vacuum bake-out prior to the Li loading. During this interval, the temperature of all wetted components must be raised in excess of the nominal operating temperature (expected during testing) of 500 °C (932 °F) to release absorbed water and other condensables from the metal.

The high vacuum is provided by a turbo pump system with an ion gauge connected to the lower and upper reservoirs. During this process, a vacuum level of 10^{-5} torr (1.93 psi), as read by the ion gauge, is targeted when the system is at the target temperature. Once the bake-out temperature is reached and maintained, the pressure will initially increase, then slowly decrease with time; sufficient time should be allowed during bake-out for the pressure to return to the low 10^{-5} torr range. After conditioning, the trace heaters are used to provide extra power to the circuit where needed. Because these heaters are operated in a vacuum, a type-K TC is embedded in the heater in order to monitor temperature and prevent burnup. The heaters were coiled around the tubing in logical division to provide some control over the application of heat. The heaters were clamped in place with hose clamps, and several layers of aluminum foil were tightly pressed around the heater and tube. The aluminum allows the heat from the portion of the heater not in contact with the tube to be dispersed more evenly about the tube. Additionally, a minimum of two layers of multilayer insulation (MLI) are stood off via wire standoffs from the tubes. This reduces radiation losses, which are the most dominant heat loss mechanism in a vacuum. Each of the components is wrapped in a similar manner—the details of which are supplied in sections 4.4–4.11.

4.4 Tilt Table

A tilt table fabricated from aluminum structural members and plating has a 2-m (6.56-ft) width and 3-m (9.84-ft) length. This table can be tilted from a level, horizontal position to an angle of 5°. The support rails are equipped with six rollers, two large hinges, and four intermediate supports (to distribute weight). Figure 8(a) shows the table during construction, and figure 8(b) shows it completed. The support table holds all components for the circuit. It is also equipped with a SS spill tray (0.25-cm (0.1-in) thick) that covers its entire surface. The tray has a 13-cm- (5.12-in-) high lip around its boundary, which is more than sufficient to contain all system Li should it leak out while the table is tilted to the maximum angle. Design drawings for the support table are located in section J of the supplemental information.

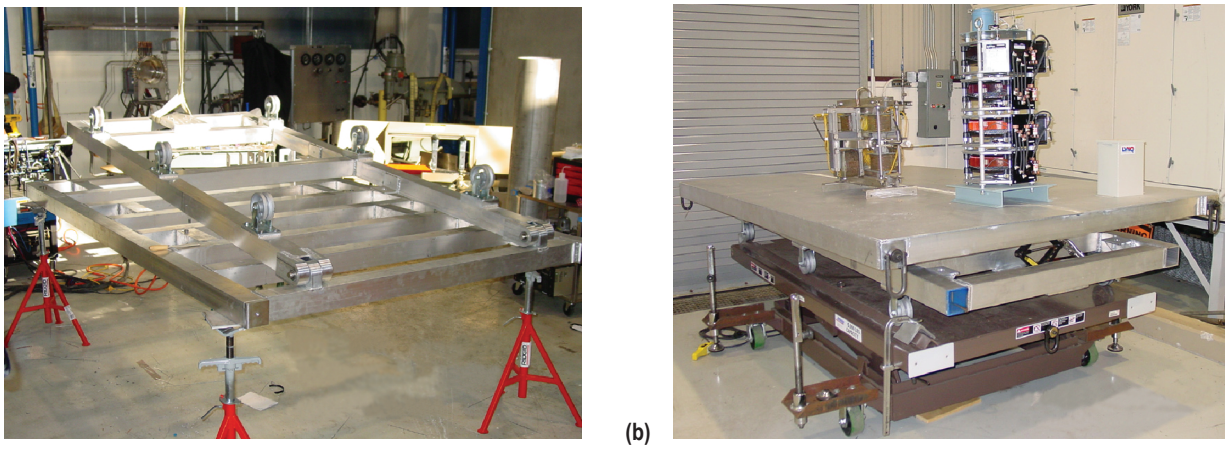

Figure 8. Tilt table: (a) During construction and (b) completed.

4.5 Core

The core assembly is oriented horizontally to simplify heater installation and to allow sufficient table tilt for complete drainage. Figure 9 provides a simplified schematic of the core block assembly, which is constructed of SS 316 (all-welded configuration) and inspected by a complete radiographic survey and He leak detection (to a level of 1×10^{-9} SCCM). The complete core assembly consists of six primary components:

(1) The core block is a solid, six-sided SS structure with 37 fuel pin holes gun-drilled through the full length of the core block. The top end is flanged to provide a support for the inlet plenum, and the backside is grooved to accept the outlet plenum cap.

(2) The outer pressure shell is a large tubular jacket that surrounds the core block (forming the perimeter flow passage). This shell is flared at the top end (using a conical reducer) to provide the inlet plenum structure. The shell length extends below the bottom of the core block, forming the outer wall of the lower manifold.

(3) The inlet plenum is an annular manifold that is part of the outer pressure shell assemblies. It is equipped with a large feed line to minimize system pressure drop.

(4) The outlet plenum is a cap structure located on the top portion of the core block assembly. This plenum is equipped with a large drain line to minimize system pressure drop.

(5) The lower manifold is formed between the lower segment of the outer pressure shell and the end of the core block. A SS faceplate (drilled to match the core block fuel pin pattern) seals the end of the manifold. This manifold receives inlet flow (from the perimeter passage) and directs it back up around the fuel pins.

(6) The fuel pin clad is a tube that is seal welded to the lower manifold and extends along the core block to the outlet plenum. (The plenum end of the tube is sealed.) Heater elements are inserted into the open tube extending beyond the lower manifold faceplate. The outer edges of the fuel-pin clad are equipped with standoffs at the center and outlet plenum end, set at 120° intervals, in order to maintain the annular flow path dimension between the core block and clad.

The complete engineering design drawings for the core assembly are located in section C of the supplemental information. The core block is held in place by a set of SS support collars that allow for thermal contraction/expansion during test operations. To minimize core heat losses during operation, the core is insulated with a set of slip-on SS MLI shields (very effective if operated in vacuum conditions). Core surface temperature measurements are made by spot welding TCs directly to the surface. There are no provisions for placing thermowells into the core block or the lower manifold because they significantly disrupt the Li flow. One thermowell is placed in the outlet plenum. Pressure transducers were purchased and are planned for placement on the inlet/outlet plenum lines and in the outer pressure shell just upstream of the lower plenum.

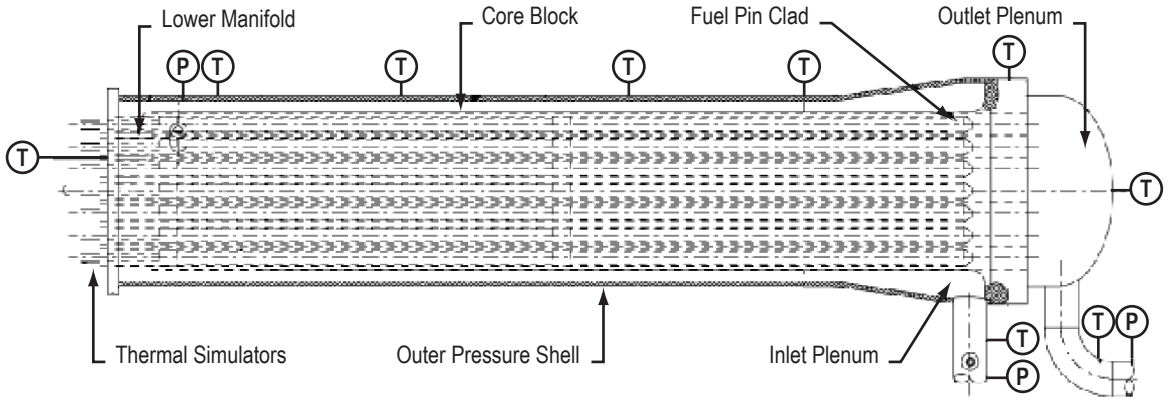

Figure 9. Simplified core assembly layout.

4.5.1 Thermal Simulators

The heater elements selected for this system were based on a graphite design that has been successfully used on a number of EFF–TF projects. The graphite heater element has a diameter of 0.775 cm (0.305 in) and an overall length of 59.7 cm (23.5 in). The heater element is equipped with alumina insulating rings that measure 1.27 cm (0.5 in) in length and have an outside diameter of 1.067 cm (0.42 in). The elements are positioned ≈4.5 cm (1.8 in) into the core as measured from the outer surface of the lower manifold faceplate. Each heater has a resistance of ≈0.9 Ω at room temperature and 0.5 Ω at an operating temperature of 700 °C (1,292 °F). Figure 10(a) is a drawing of one of these heaters, and figure 10(b) is a photograph of the heaters.

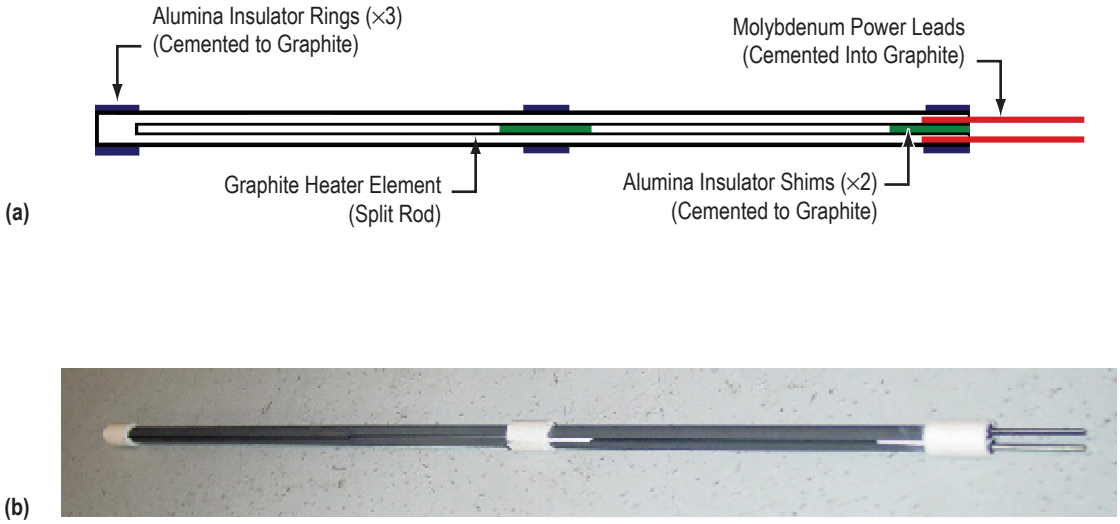

Figure 10. Thermal simulators (heaters): (a) Drawing and (b) photograph.

4.5.2 Power Zones

The baseline approach requires that heaters be assembled in zones that are connected to individual power supplies (one power supply per zone). Each power supply is rated for 15 kW of direct current power delivered via 150 V at 100 A maximum. The 37-pin core assembly is divided into three control zones, as depicted in figure 11. The grouping of heaters in these zones (series/parallel) is laid out such that the equivalent resistance attempts to maximize the power supply output capability.

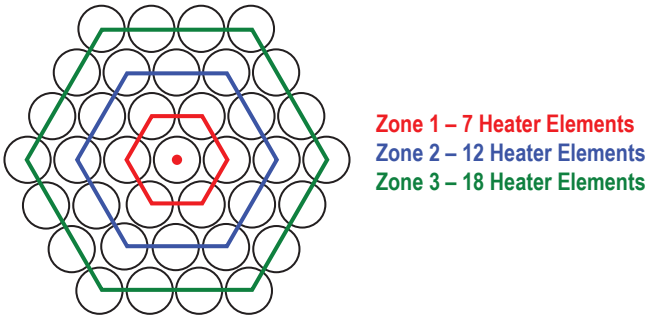

Figure 11. Heater element layout and heater zone configuration.

Table 2 lists the estimated equivalent resistance per zone and the maximum power that can be transferred by the power supplies with the heaters at room temperature and at nominal operating temperature. The central zone could be split into two parallel circuits producing an equivalent resistance of 1.2 Ω and resulting in a total power of 11.66 kW at 700 °C (1,292 °F). The total available input power would then be 41.66 kW at 700 °C (1,292 °F). If additional power is required (to simulate transients), more power supplies could be added to create additional zones. To match the power supply load for maximum output, a load of 1.5 Ω is desired; therefore, a maximum of 12 zones could be created (approximately three heaters per zone) resulting in a total available input power of 180 kW.

Table 2. Heater zone configuration.

Power Supply Parameters									
Heater Ring	Number Heaters	Res/Heater @ 25 °C (77 °F) (Ω)	Res/Heater @ 700 °C (1,292 °F) (Ω)	Number Parallel Heater Strings	Number Heater Per String	Load @ 25 °C (77 °F) (Ω)	Load @ 700 °C (1,292 °F) (Ω)	Max Power @ 25 °C (77 °F) (W)	Max Power @ 700 °C (1,292 °F) (W)
1	7	0.9	0.5	1	7	6.3	3.5	3,571	6,429
2	12	0.9	0.5	2	6	2.7	1.5	8,333	15,000
3	18	0.9	0.5	3	9	2.7	1.5	8,333	15,000
							Total	20,238	36,429

Note: Assumes one 15-kW power supply per zone (150 V (max), 100 A (max)).

4.5.3 Face Seal

To improve the thermal performance of the 37-pin Li system there is a core face sealing assembly. This assembly, which is attached to the power inlet end of the core, allows for a He environment to be established between the fuel cladding and the heater, significantly improving the overall thermal conductivity (coupling) between the heaters and core clad. This better simulates the thermal conditions in the actual core in which GHe within the fuel pin provides excellent heat transfer across the pin. Figure 12 illustrates this concept. The core face sealing assembly is connected to the main core body by a 16.24-cm- (6-in-) diameter ConFlat® (a Varian, Inc. product) flange (shown as a weld in fig. 13) and a second 16.24-cm- (6-in-) diameter ConFlat flange to rear access flange. These flanges use a two ConFlat type sealing surface and

a Ni seal, allowing for operation up to 500 °C (932 °F). A series of vacuum-rated power feedthroughs are seal welded to the perimeter of the seal assembly and connected to the heater elements through the rear access flange. One flange provides the rear access and the other provides the connection to the core. To reduce the amount of heat conducted out of the face seal assembly, an area of the assembly barrel is turned down to a thickness of 0.05 cm (0.02 in) or less, which still provides sufficient mechanical strength, yet reduces the cross-sectional area for heat transfer. In addition, a series of perforated stainless foil shields (three to five) are mounted over the heater leads (using alumina spacers for insulation) to provide a thermal radiation barrier. The outer diameter of the assembly matches that of the core outer pressure shell, while its length 20 to 30 cm (7.87 to 11.81 in) allows sufficient standoff length from the core so that the rear access flange temperature is maintained well below 500 °C (932 °F).

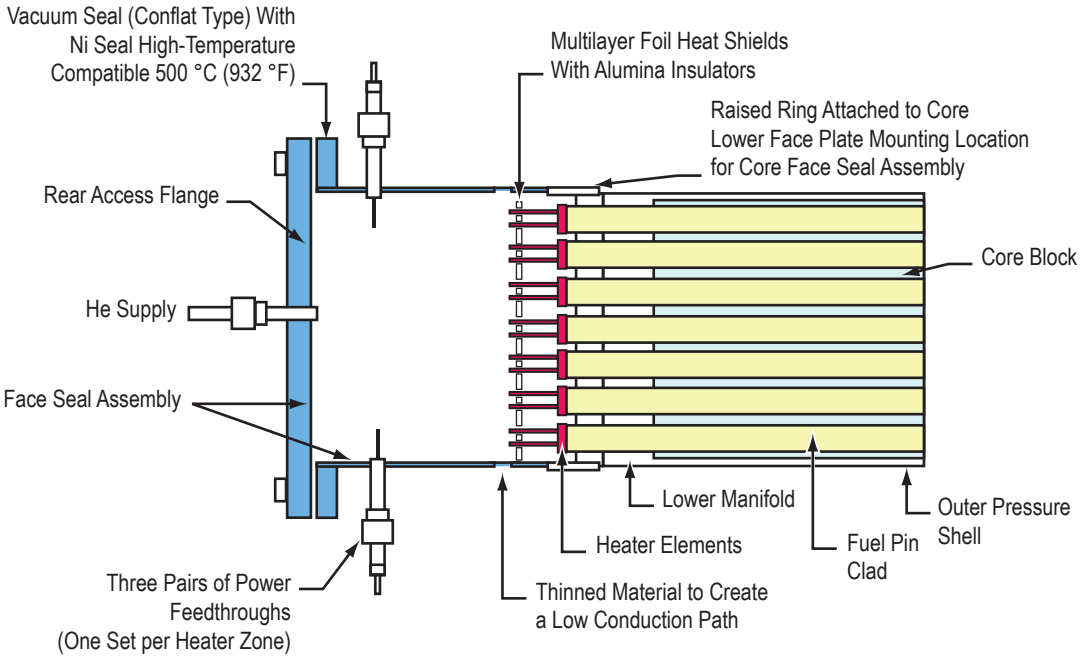

Figure 12. Simplified schematic core face sealing system.

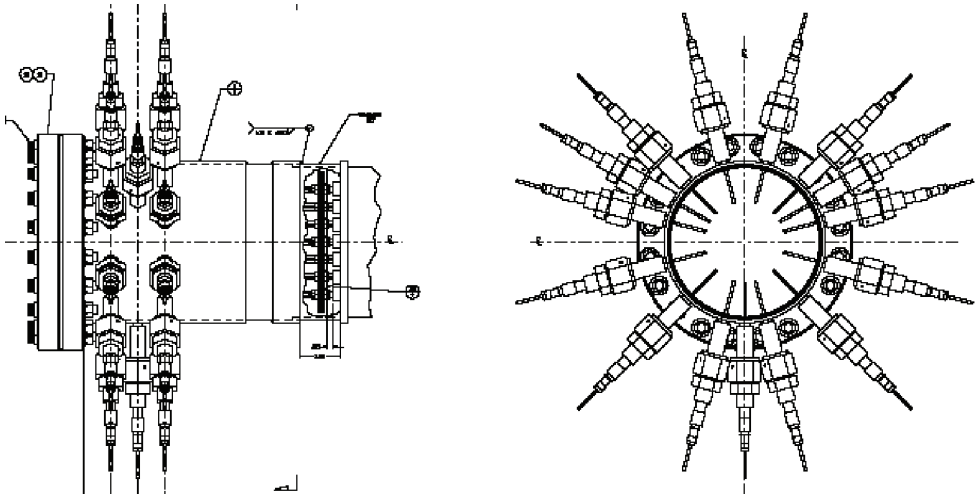

Figure 13. Drawing of core face seal.

4.6 Heat Exchanger

Once the Li coolant is heated by the core assembly to a temperature of ≈500 °C (932 °F), it passes into a HX to remove up to 40 kW. The baseline for this HX was a 'battleship' or facility-style design that provides significant robustness in this initial flow circuit (see fig. 14). It is a 0.6-m- (1.97-ft-) long counter flow design with Li confined by the outer jacket (14.1-cm (5.56-in) outer diameter) and the secondary coolant flow (a gas, either HeAr or N_2, in this application), confined by 107 tubes (0.8-cm (0.32-in) outside diameter) that pass through the Li flow pool. Engineering drawings for this HX and its high temperature gas feed lines are presented in sections A and D of the supplemental information. The exchanger is equipped with temperature and pressure measurements to monitor material and fluid conditions. Two 165.1-cm- (65-in-) long, 240-V, 675-W Watlow cable heaters were positioned on the HX to provide heat during a thaw

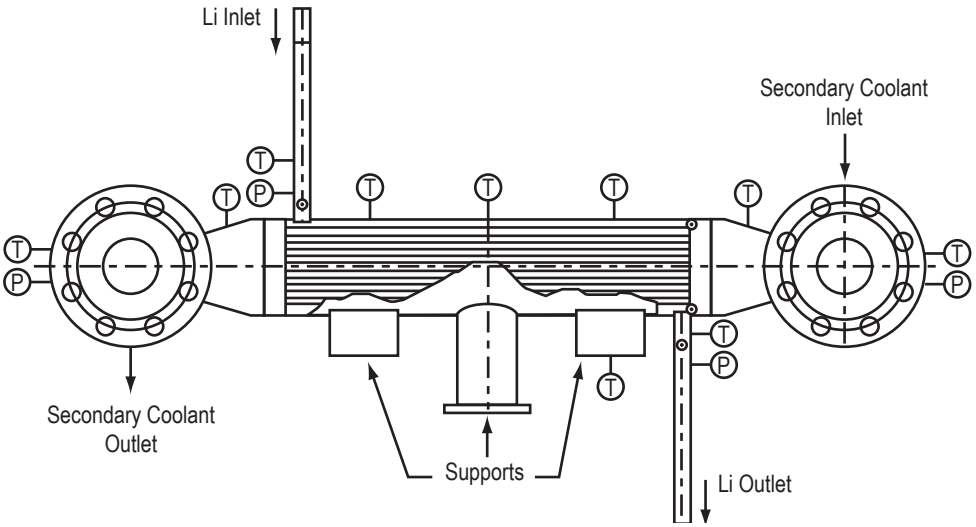

Figure 14. Lithium/HeAr HX unit.

startup condition, or as needed during filling or transient operations. It is not anticipated that these trace heaters would be required during steady-state operations. One trace heater was positioned on the top and one on the bottom of the HX (see fig. 15). Each heater has two TCs positioned between the trace heater and the HX body to provide feedback temperatures for automatic control of the system. Figures 15 and 16 illustrate the position of the top heater TCs (THTCs), which are identified as THTC1 and THTC2, and the bottom heater TCs (BHTCs), BHTC1 and BHTC2. Additional type-K TCs, TC1 through TC8, are spot welded at various locations around the body, as indicated in the figures, to provide temperature information. The affixed trace heaters and TCs are then wrapped with 0.076-mm (0.003-in) copper foil to aid in thermal conduction from the trace heater to the body (see fig. 17). Any gaps between the trace heater and the core body would result in localized heating of the trace heater and this excess temperature could result in trace heater failure. Additionally, the copper wrap allows the trace heater to grow and contract as needed due to the differing rates of expansion caused by the temperature difference between the trace heaters and the HX. The two options for the secondary coolant flow on this heat exchange include:

- A closed-loop He system that can provide flow rates up to 0.2 kg/s (7.06 oz/s), operating pressure up to 1.4 MPa (203.1 psi), and inlet temperatures up to 490 °C (914 °F). Maximum loop pressure is 2.4 MPa (348.1 psi); however, system temperature must be reduced to maintain sufficient material strength margins.

- A single-pass, gaseous N_2 (GN_2) configuration that can provide 1.4 MPa (203.1 psi), at flow rates in excess of 0.4 kg/s (14.11 oz/s), and inlet temperatures of 490 °C (914 °F). The heated exhaust gas is vented to the atmosphere.

Section 5 discusses the network flow model developed to calculate the required flow rates.

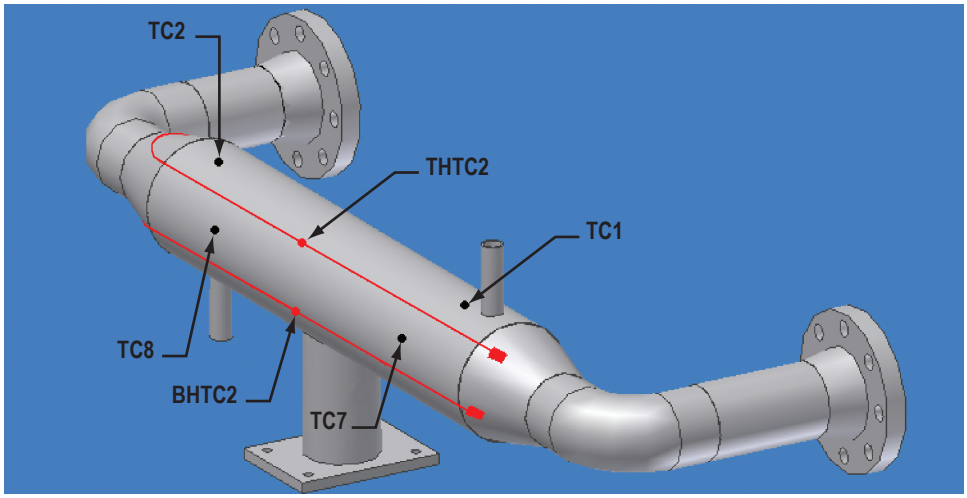

Figure 15. Back view of a HX.

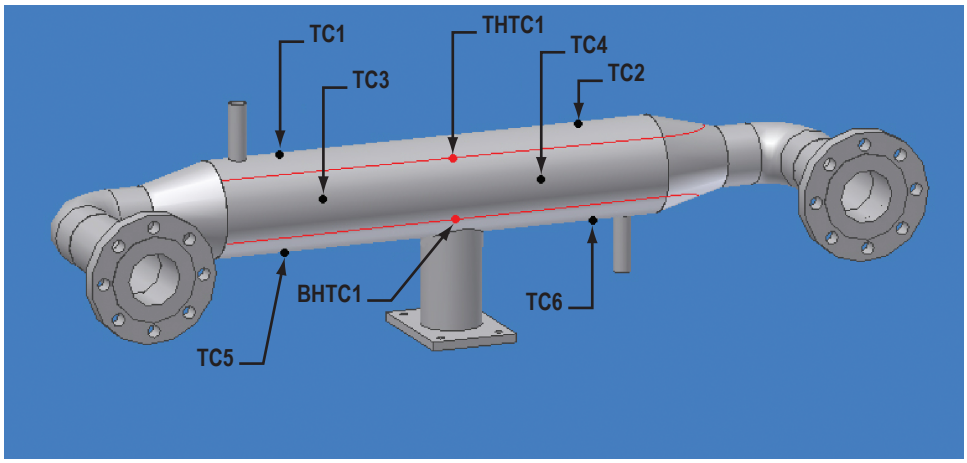

Figure 16. Another back view of a HX.

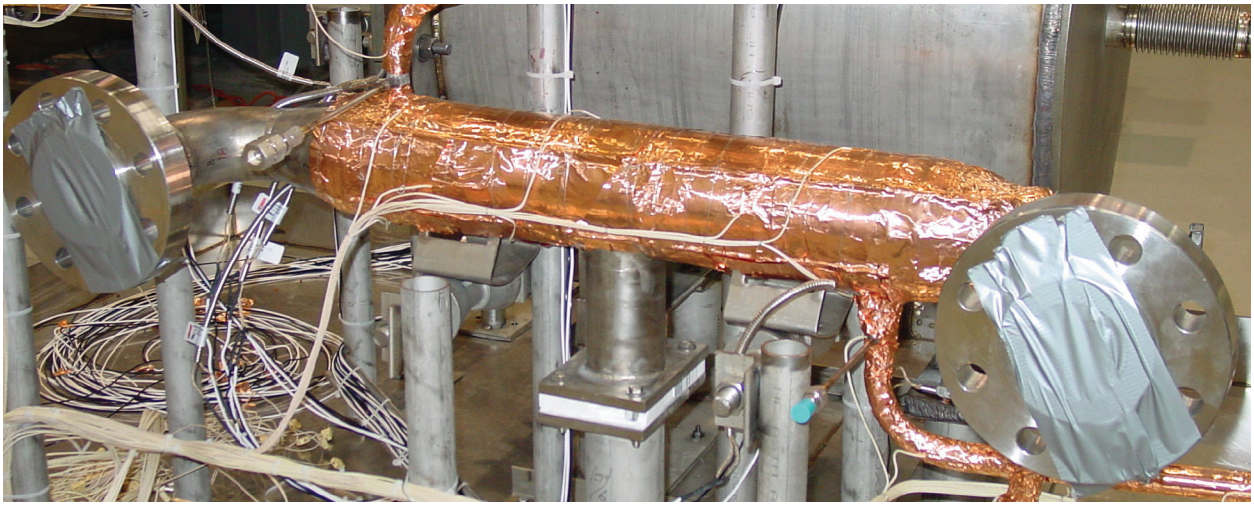

Figure 17. Build view of a HX showing Cu foil wrap.

During the HX design, an analysis was performed to assess its performance over 0.6- and 1.2-m lengths, for various secondary coolant gases (He, HeAr, and N_2) and at various flow rates. The description and results of this analysis are provided in section K of the supplemental information. To minimize heat losses from the HX, the next step (not shown) was to cover the unit with MLI radiation shielding (layers of aluminum foil) and to use alumina isolation standoffs from the support structure.

4.7 Pump

An electromagnetic (EM) pump was selected as the baseline in order to maintain the integrity of the all-welded flow loop with no moving parts and to build experience with a pump type that is applicable to a space power system. A general product search and open procurement in the commercial market resulted in a single pump submission that met the flow, temperature, and pressure requirements. The pump is a Style-VI, two-stage ac conduction unit with a SS 316 duct originally marketed by Mine Safety Appliance and currently offered by Creative Engineers, Inc. (The design dates back to the 1950s.) This pump makes use of commercial windings. Figure 18(a) shows the pump system (protective shielding removed) before integration into the pump housing. Figure 18(b) shows the three-phase auto transformer. This pump provides continuous operation at temperatures up to 816 °C (1,501 °F), with flow control from 10% to 100%. Control is provided by a three-phase, motor-driven variable transformer.

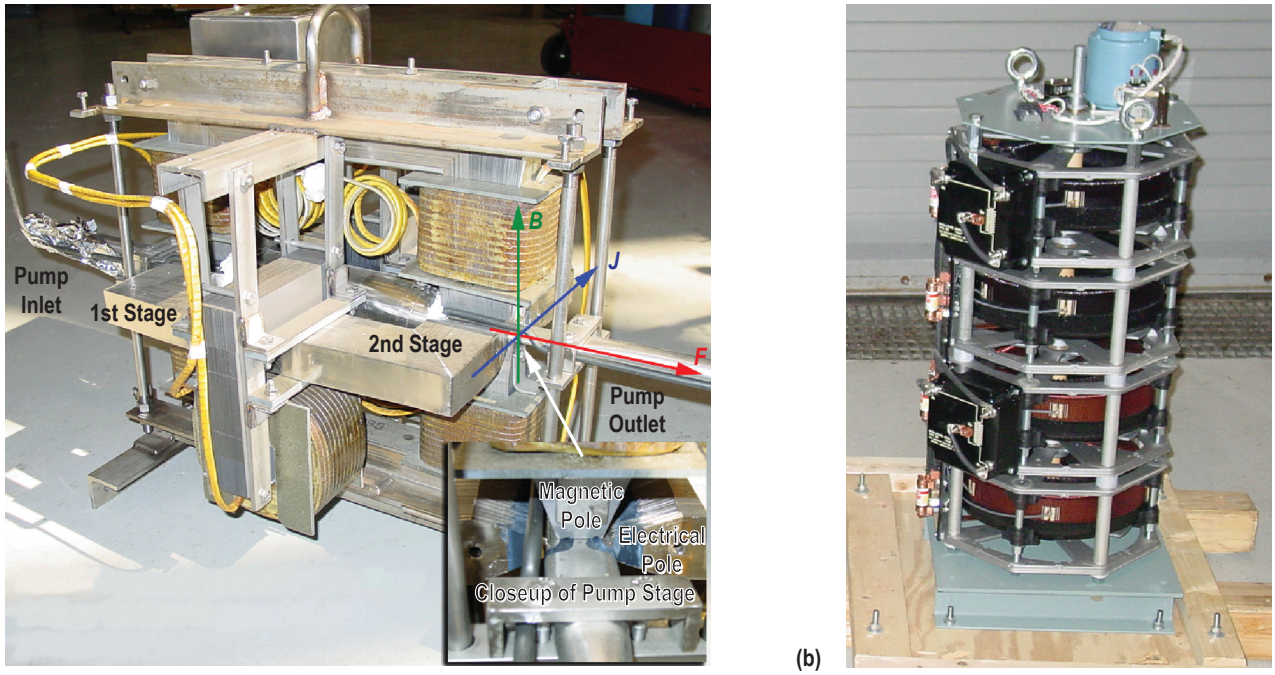

Figure 18. Style-VI: (a) ac conduction pump and (b) three-phase autotransformer.

The Style-VI pump makes use of a flattened flow duct in the pumping stages; therefore, the pressure differential across the piping is limited to prevent circularization of the duct and pump failure. The maximum allowable pressure differential as a function of temperature is shown in figure 19 (data supplied by manufacturer). Nominal operation of the 37-pin system will require a pressure differential (relative to vacuum) of ≈20.3 psi (≈140 kPa). This pressure drop is within the pump's limits.

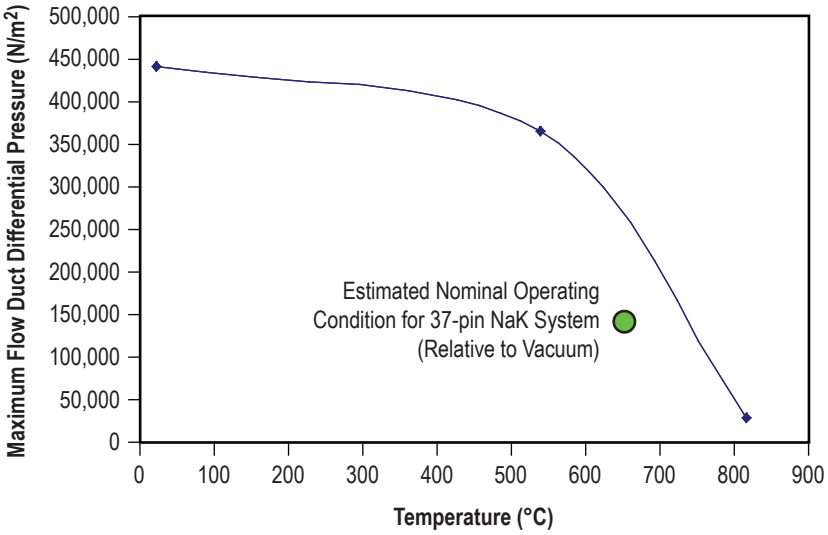

Figure 19. Style-VI pump flow duct maximum differential pressure. (Exceeding this limit will result in circularization of the flat pump duct.)

The Style-IV pump performance for NaK-56 alloy is shown in figure 20. The expected nominal flow and pressure differential required to operate the 37-pin NaK flow loop is shown by the data point in the figure. Currently there are no pump performance curves for Li, but this figure provides a basis for making an educated guess as to the pump performance with Li. The manufacturer of the pump has expressed a desire to gather data from this testing.

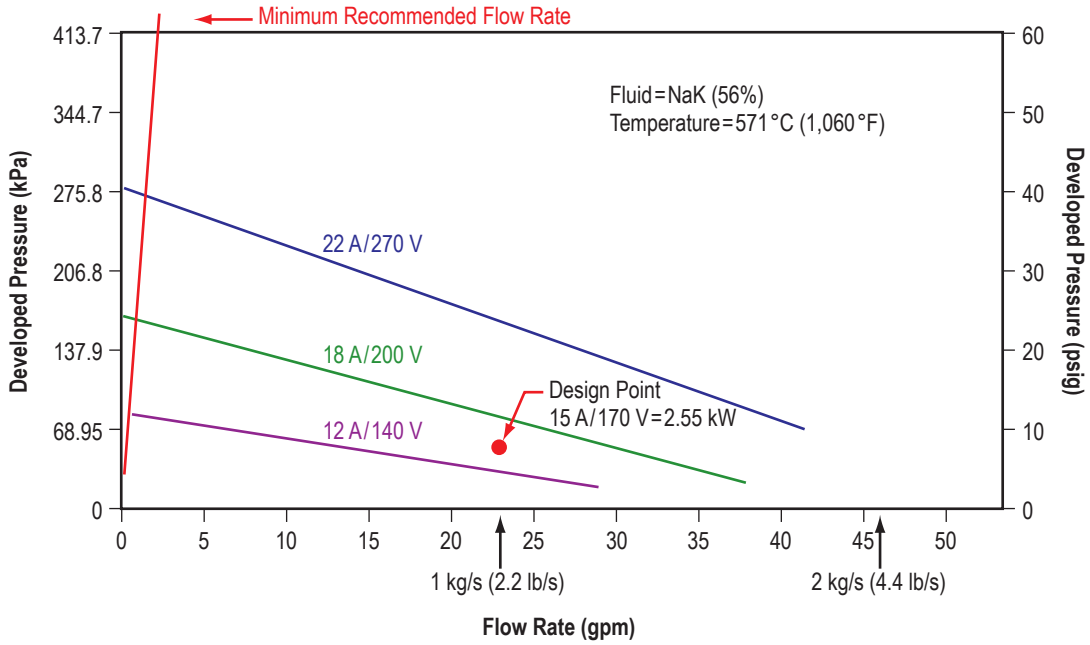

Figure 20. Style-VI ac conduction pump performance curve. (Reproduced from MSA Research Corp. Dwg. No. C-510356.)

4.8 Pump Housing

Because of the heat generated by the pump and the temperature limitation of the commercial magnet coils, a SS pump enclosure has been designed so that a GN_2 cooling purge can be provided to the unit during high-temperature operation (fig. 21).

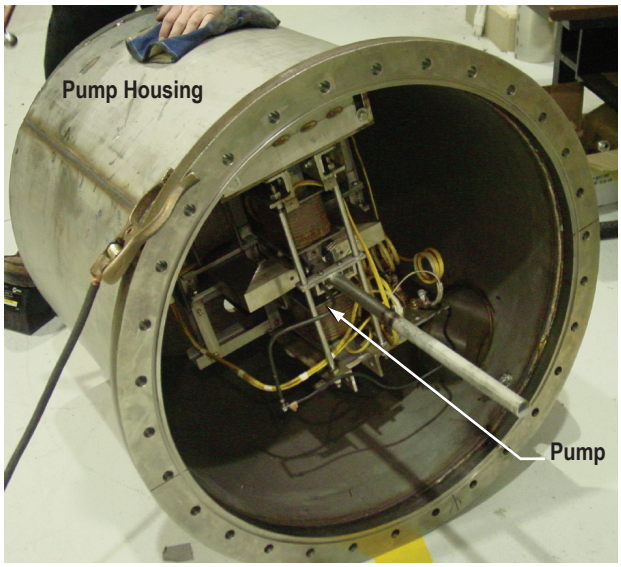

Figure 21. Pump housing with pump mounted inside.

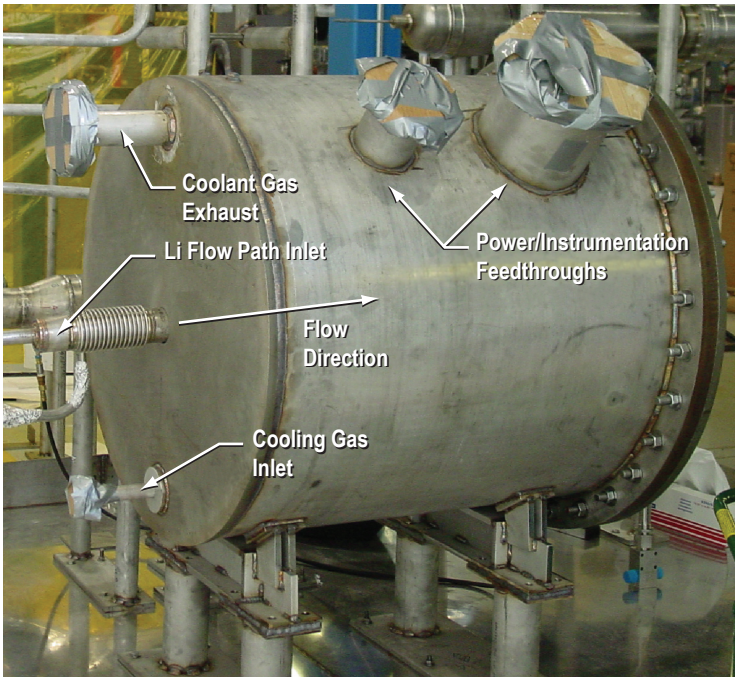

Figure 22. Pump housing viewed from outside.

The pump enclosure is necessary because the entire system will be placed in a vacuum chamber with pressure conditions of 10^{-5} torr or lower, eliminating natural convective cooling of the pump. The pump enclosure was purged with N_2, providing necessary cooling for the pump. The pressure vessel has a maximum pressure rating of 290 kPa (42 psia). Failure of the pressure vessel could result in catastrophic failure of the liquid metal system because the pressure vessel is welded directly to the Li flow lines via expansion bellows. To ensure that this maximum pressure cannot be exceeded, pressure relief valves were set at 241 kPa (35 psia) such that system operating pressure can never exceed 241 kPa. Nominal operating pressure was set at 172 kPa (25 psia); however, because this is an open cycle system venting to atmosphere (100 kPa (14.5 psia)), this leaves an ≈69 kPa (≈10 psi) pressure differential available between the pump housing pressure and atmospheric pressure (outside the building). Calculations, detailed in section L of the supplemental information, indicated that 5.08-cm- (2-in-) diameter exit lines would be required to allow a minimal pressure drop to satisfy the pressure drop constraint (fig. 22). The drawings for this enclosure are provided in section E of the supplemental information. An initial estimate of the N_2 flow rates for various heat loads was performed; results are shown in figure 23.

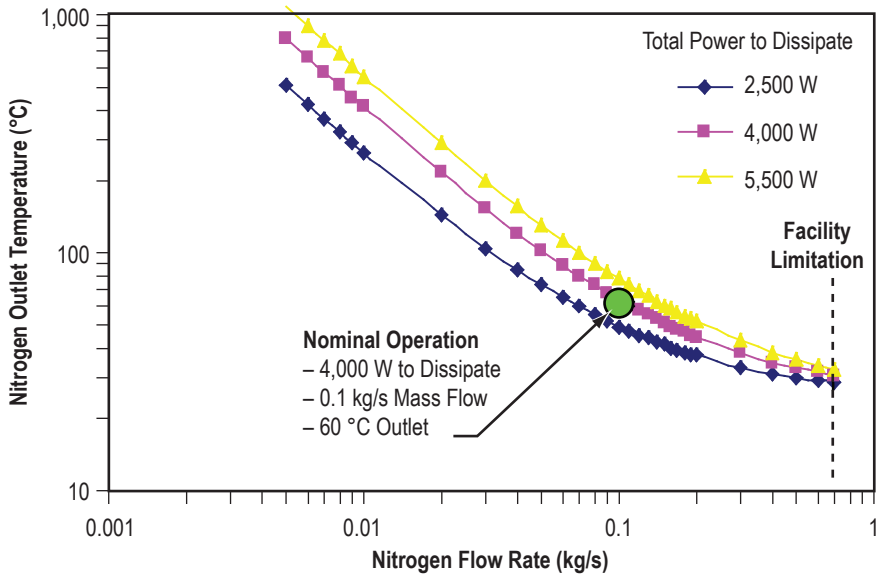

Figure 23. Pump enclosure coolant performance curves.

The total power to dissipate includes the pump excess (≈2,500 W) that is lost through the pump duct insulation. There is ≈1 m (≈3.28 ft) of pump duct within the enclosure, transferring ≈1,500 W (duct assumed covered with an Insulfrax® blanket (a Unifrax Corp. product)). The resulting load on the cooling system is ≈4,000 W. The facility N_2 supply temperature varies from 25 °C (77 °F) at low flow rates to 0 °C (32 °F) at high flow rates (flow cools as it expands through regulators; line pressure is reduced from 10.34 to 0.14 MPa (1,500 to 20 psi)). The selected operating point provides a coolant mass flow of 0.1 kg/s (3.53 oz/s), an inlet temperature of 25 °C (77 °F), and an outlet temperature of 70 °C (158 °F).

4.9 Lower Reservoir

A lower reservoir (LR) is placed at the lowest elevation of the system to serve as a storage vessel for both the fill and drain operations. The LR also serves as the storage tank for the Li between tests. After the system has been baked out, the Li will be loaded molten from the fill pot in the tube shown in figure 24. Once loading from the fill pot tube is completed, this tube would be connected to a pressurization system that would supply low pressure Ar, measured with an Astro sensor pressure gauge located at LRPG1. During fill operations, applying pressure to the top of the liquid metal will force the liquid up and into the evacuated tubes of the circuit via the to/from circuit tube that extends to the bottom of the LR. The fill/drain valve (a Swagelok SS–12UW series valve using a series 8 actuator, not shown) located between the LR and the circuit on the to/from circuit tube (fig. 24) was specified for remote operation. However, procurement of this valve and actuator was stopped before delivery. Section M in the supplemental information contains the specifications for this remote operated valve (ROV) kit.

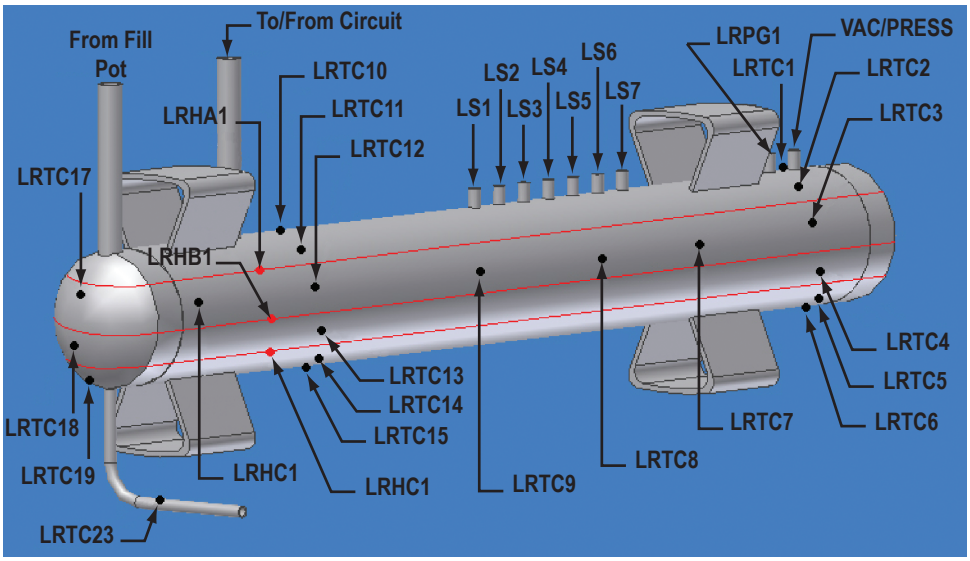

Figure 24. Lower reservoir instrumentation and trace heater location—front view.

The entire reservoir was wrapped with copper foil to aid in thermal conduction and to avoid trace heater burnup; however, this will tend to flatten the thermal gradients produced from the trace heaters and may retard some of the thermal control of the freeze/thaw process.

High-temperature valves, used to drain the circuit reservoir, were placed at the lowest elevation (fig. 5). The selected valves are all SS bellows suitable for a maximum operating temperature of 650 °C (1,202 °F).

This reservoir is equipped with two blocking valves, level sensors, TCs, trace heaters, and a purge line to assist in fill and drain operations. A Li melt pot (with its own pressurization system) is coupled to the LR for the initial fill.

4.9.1 Trace Heaters

Three 2.36-m- (93-in-) long, 240-V, 1,000-W Watlow cable-type trace heaters (LRHC1, LRHB1, LRHA1) were positioned on the LR (figs. 24 and 25) to provide the heat that will be required to melt the Li before introduction into the system for a test. The trace heater locations were selected in an attempt to provide some control over the heating profile. Void formation in the LR will occur at the top of the reservoir due to gravity; therefore, controlled freeze/thaw is desirable and can be accomplished using the trace heaters in a specified configuration.

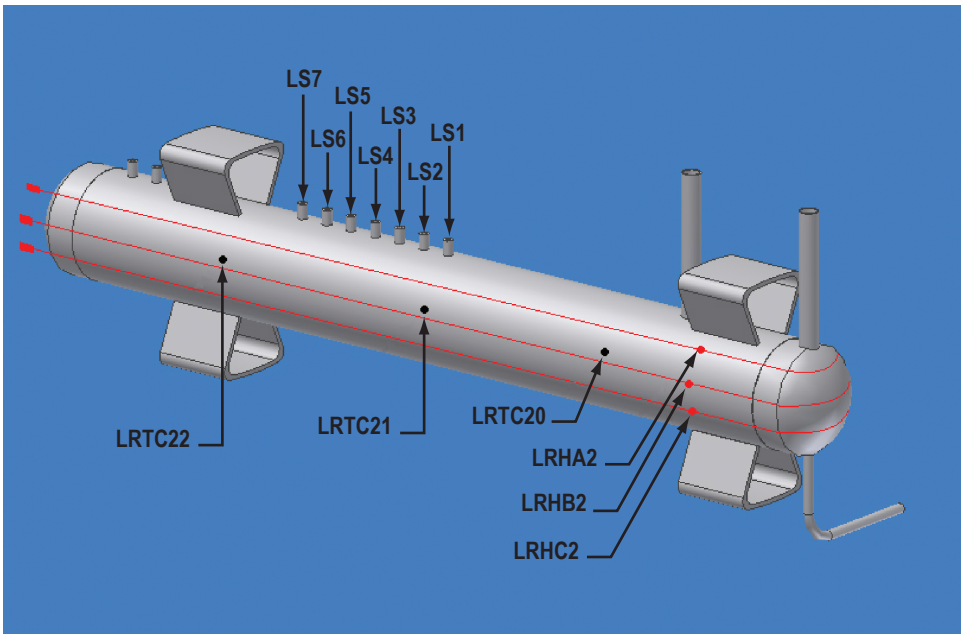

Figure 25. Lower reservoir instrumentation and trace heater location—rear view.

4.9.2 Thermocouples

There are 23 TCs (LRTC1–LRTC23) spot welded to the LR. In addition to providing bulk temperature data, LRTC1–LRTC6 and LRTC10–LRTC15 were placed to provide a second method of level sensing. In earlier experimentation with Li at elevated temperatures, it was observed that the skin temperature of the vessel quickly normalizes when Li is present on the opposing side.

4.9.3 Level Sensors

The level sensors, described in section 4.2.3, were installed in the LR as shown in figure 26. This sensor uses a single SS pin; only the sensor pin comes in contact with the liquid metal. The ceramic insulating material used in the feedthrough is several inches above the height of the liquid metal, such that it should never come in contact with the Li. Sensor LS7 was intended as a high-level indicator from which a shutdown procedure could be initiated. The level sensor lengths were sized to provide readings of the Li at the levels indicated in figure 27. The system functions by using one sensor, LS1, as the common ground;

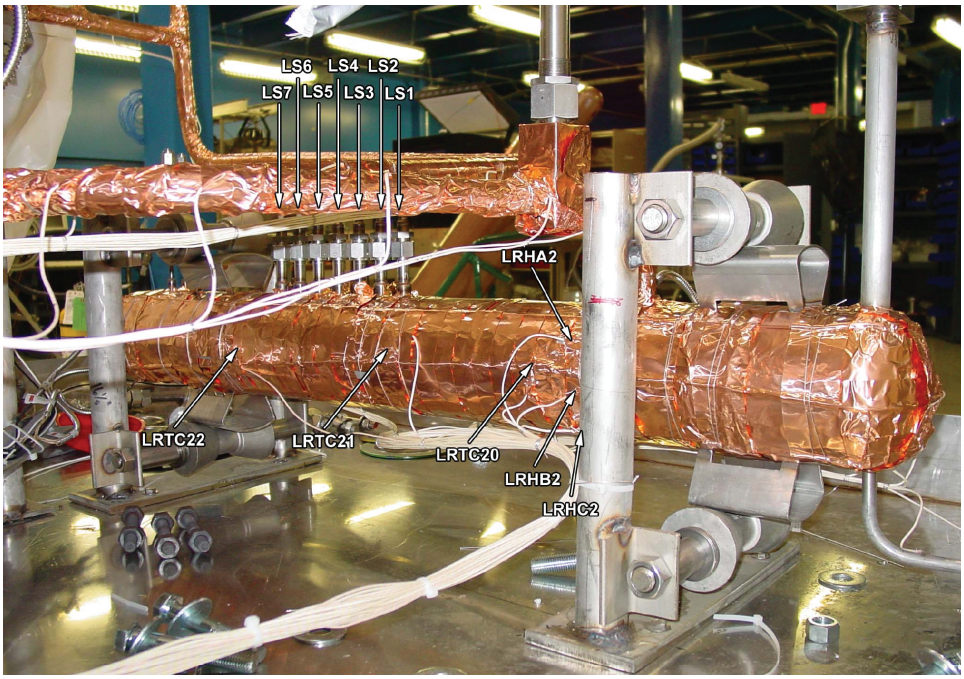

Figure 26. As-built view of the LR.

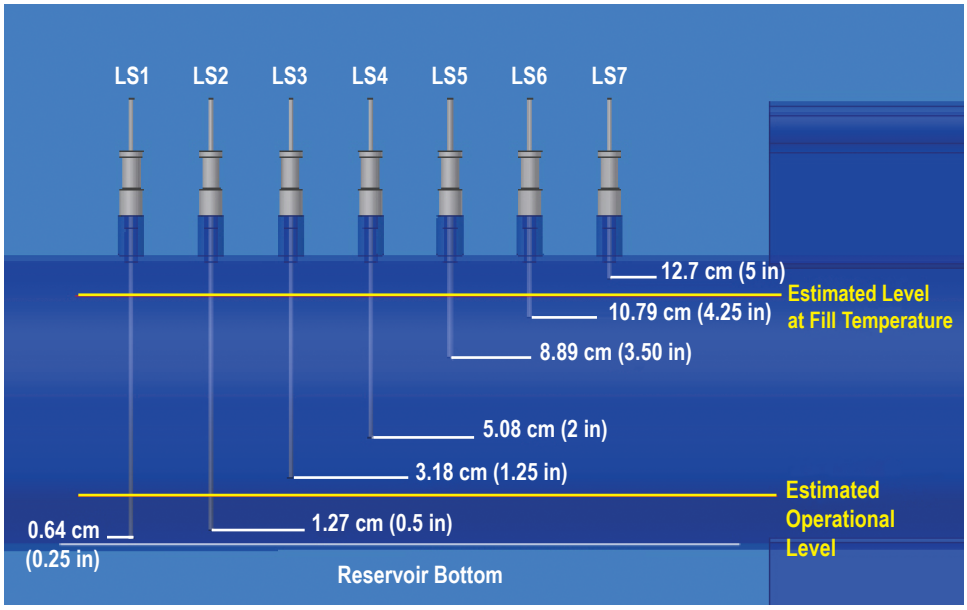

Figure 27. Level sensors to detect Li fill level in the LR.

the balance of the sensors complete a circuit to indicate fill level in the presence of the Li. Calculations indicate that the Li will rise to a height between LS6 and LS7 at the fill temperature, ≈250 °C (482 °F).

4.10 Upper Reservoir

Because the fill/drain reservoir was relocated to the lowest height in the circuit, additional volume, the upper reservoir (UR), was required to accommodate the difference in thermal expansion of the Li between the fill temperature, ≈250 °C (≈482 °F), and the operational temperature, ≈500 °C (≈932 °F). This required volume is located at the highest point in the system. During operation, the top of the UR would be pressurized with ultra-high-purity Ar (at relatively low pressure) to maintain a pressure head on the system to prevent the EM pump from oscillating rather than circulating. This same pressurization system was also intended for use in drain procedures to drive the Li out of the UR. Figures 28 and 29 show the placement of trace heaters and instrumentation on the UR. The entire UR was wrapped with copper foil to aid in thermal conduction and to avoid heater burnout, as shown in figure 30.

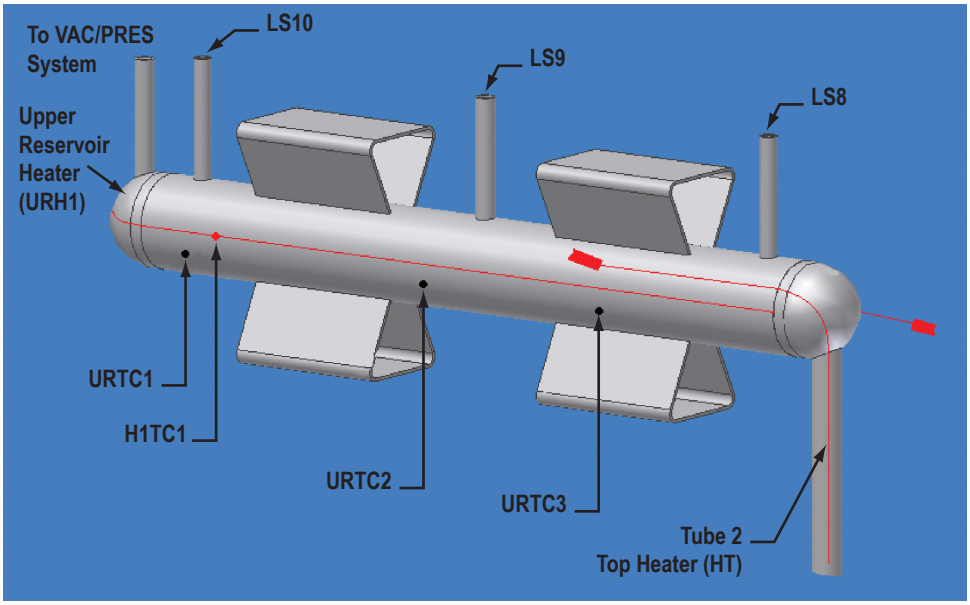

Figure 28. Front view of the UR.

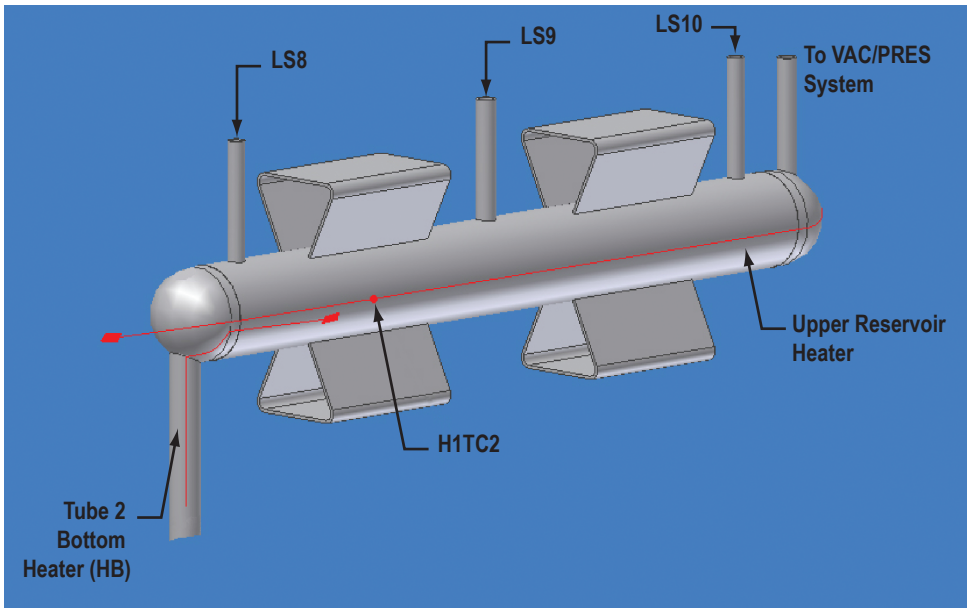

Figure 29. Rear view of the UR.

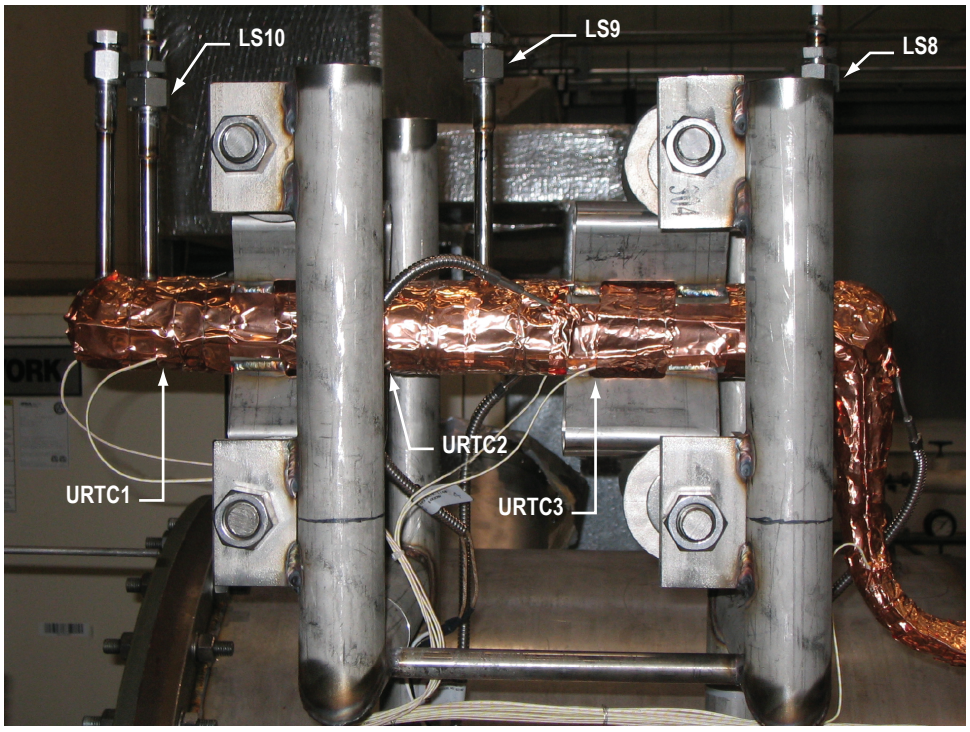

Figure 30. As-built view of the UR.

4.10.1 Trace Heaters

One 1.19-m- (47-in-) long, 240-V, 345-W Watlow cable type trace heater (H1) was placed on the UR to replace the thermal power that is lost to the environment and to provide control during freeze and thaw experiments.

4.10.2 Thermocouples

There are three UR TCs (URTC1–URTC3) spot welded to the UR, providing gross temperature data for monitoring or debugging. Two TCs are mounted directly underneath the trace heater, H1TC1 and H1TC2.

4.10.3 Level Sensors

The level sensors, described in section 4.2.3, were installed in the UR locations as shown in figure 29. Sensor LS8 was intended as a high-level indicator, LS9 the low-level indicator, and LS10 as the common ground. See figures 28–30.

4.11 Tubing

The circuit tubing is formed from seamless 316 SS tubing with a 0.24-cm (0.095-in) wall. The tube is formed per the engineering drawings, providing the system with the required flexibility; however, most of the manufacturing, fabrication, and assembly tolerances are taken up in the final fit assembly. This tubing connects all the components of the circuit; 1-in VCR fittings are used to connect and disconnect tube 4 (fig. 5) from the system. These connections define the connection points for a test section where test articles could be attached and would be available to mate any components to the circuit in the component test bypass area. Thermocouples were attached every 15.24 cm (6 in) along the length of each tube. Two heaters were attached to each tube, placing one on the top surface and one on the bottom surface to allow for controlled freeze/thaw, forcing the void space to the top. However, since the copper foil was required to disperse the heat from the heaters to avoid burnup and to allow the heaters to expand and contract at different rates than the underlying tube, the ability to control the input thermal gradient to the tube was reduced due to the superior thermal conductivity of Cu.

Heater failure occurred in early tests conducted in a vacuum environment (fig. 31). This failure was attributed to the welding tabs used to affix the trace heaters to the tubes. The intent of these tabs was to maintain good contact between the tube and the heater. If the heater did not come in contact with the tube, it would have limited paths to give off its energy and would quickly exceed its design temperatures in a vacuum. These tabs solved the thermal conduction problem but introduced the problem of differing thermal expansion rates. The heater heats and cools on a much shorter time scale than the underlying tube. By firmly affixing the heater to the tube, these differing rates of thermal expansion and contraction resulted in the heater separating from the tube, most likely on cooldown.

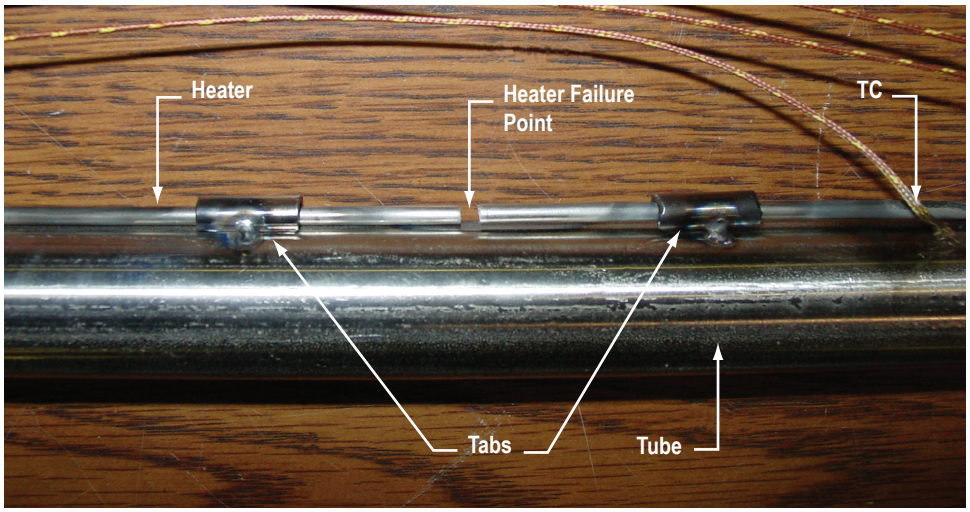

Figure 31. Photograph of heater failure using tabs to secure to tube.

These results indicated that the heater must be allowed to 'slip' yet still transfer its thermal energy to the tube. This was accomplished by using Cu foil wrapped around the tube, the trace heater, and the TCs. Figure 32 shows the test specimen with some of the foil removed.

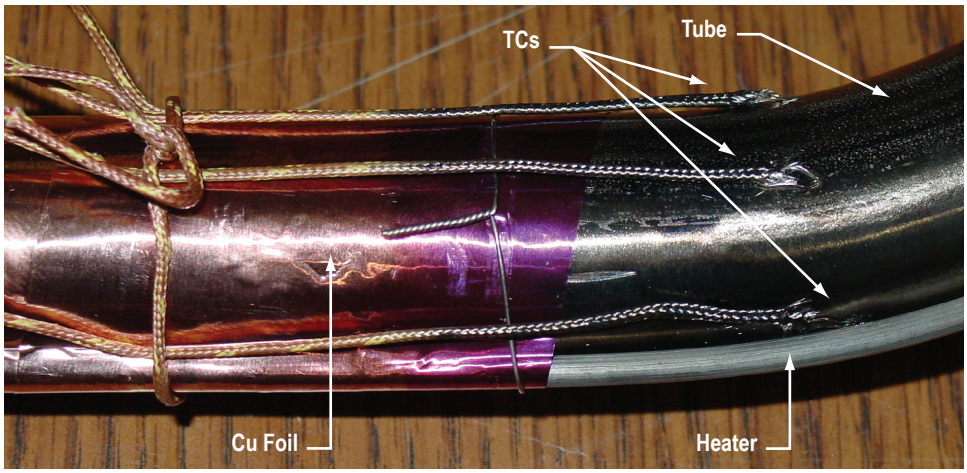

Figure 32. Photograph of successful method of securing heater with Cu foil.

The 0.008-cm- (0.003-in-) thick, 5.08-cm- (2-in-) wide Cu foil allowed the heater to slip and grow. When the heater separated from the tube due to expansion or contraction, it would still conduct the thermal energy from the heater to the tube. This system worked very well; however, it limits the ability to apply a strong, directed thermal gradient to the tube or other component, thus limiting the ability to control the freeze or thaw void placement. Despite this drawback, this was determined to be an acceptable solution for this flow circuit.

4.11.1 Tube 1

Tube 1 (T1) was instrumented with 16 TCs (T1TC1–T1TC16) that record the Li temperatures as it moves from the core to the HX. Pressure measurements are made at P1 and P2. T1H1A, T1H1B, T1H2A, and T1H2B denote TCs that are located underneath heaters T1H1 and T1H2. Heater T1H1 traces the top of the tube while T1H2 traces the bottom of the tube (fig. 33).

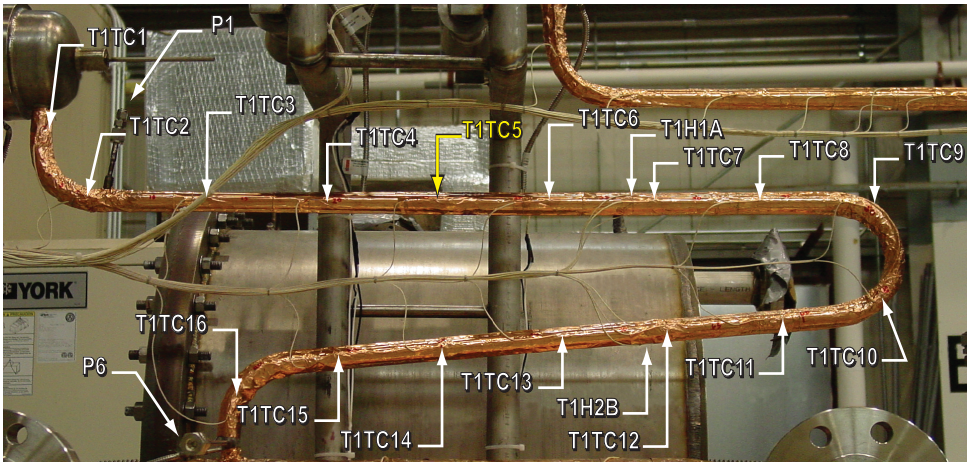

Figure 33. Photograph of T1.

4.11.2 Tube 2

Tube 2 (T2) was instrumented with 14 TCs (T2TC1–T2TC14) that record the temperatures of the stagnant Li from the main loop to the expansion tank or the upper reservoir. The Li is not flowing in this section of T2, but the TCs can be used as level indicators. The successful use of these TCs as level indicators remained to be determined. T2HT1, T2HB1, T2HB2, and T2HT2 denote TCs that are located underneath heaters T2HT and T2HB. Heater T2HT traces the top of the tube while T2HB traces the bottom of the tube (fig. 34).

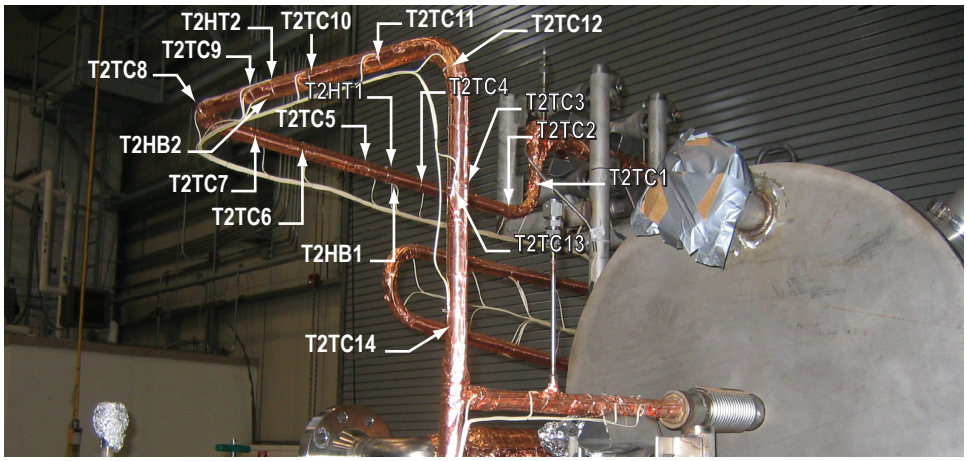

Figure 34. Photograph of T2.

4.11.3 Tube 3

Tube 3 (T3) was instrumented with 16 TCs (T3TC1–T3TC16) that record the Li temperatures as it moves from the HX to the pump. Pressure measurements are made at P1 and P2 (not shown). T3H1A, T3H1B, T3H2A, and T3H2B denote TCs that are located underneath heaters T3H1 and T3H2. Heater T3H1 traces the top of the tube while T3H2 traces the bottom of the tube (fig. 35).

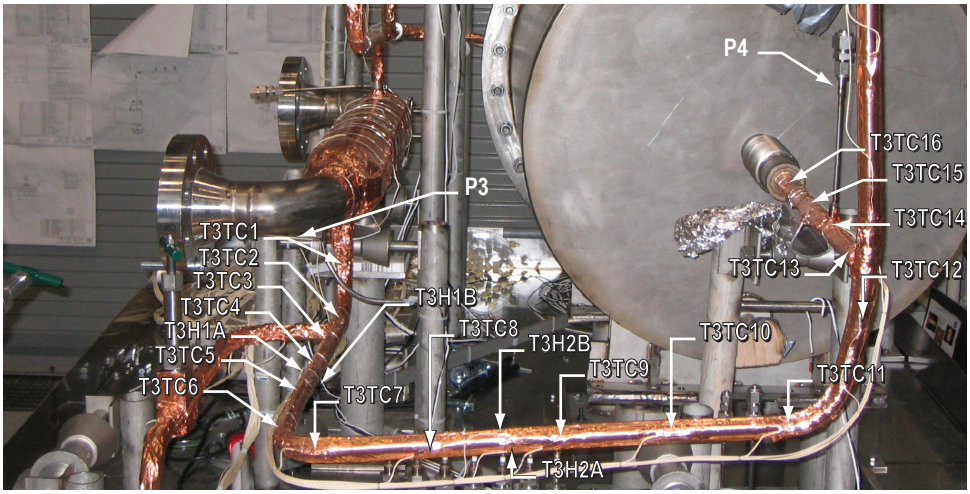

Figure 35. Photograph of T3.

4.11.4 Tube 4

Tube 4 (T4) was instrumented with six TCs (T4TC1–T4TC6) that record the Li temperatures as it moves from the pump to tube 5 (T5) and ultimately to the core. A pressure measurement is made at P5. Thermocouple T4H1 is located underneath heater T4H1. Only one heater, T4H1, spirals around the tube section (fig. 36).

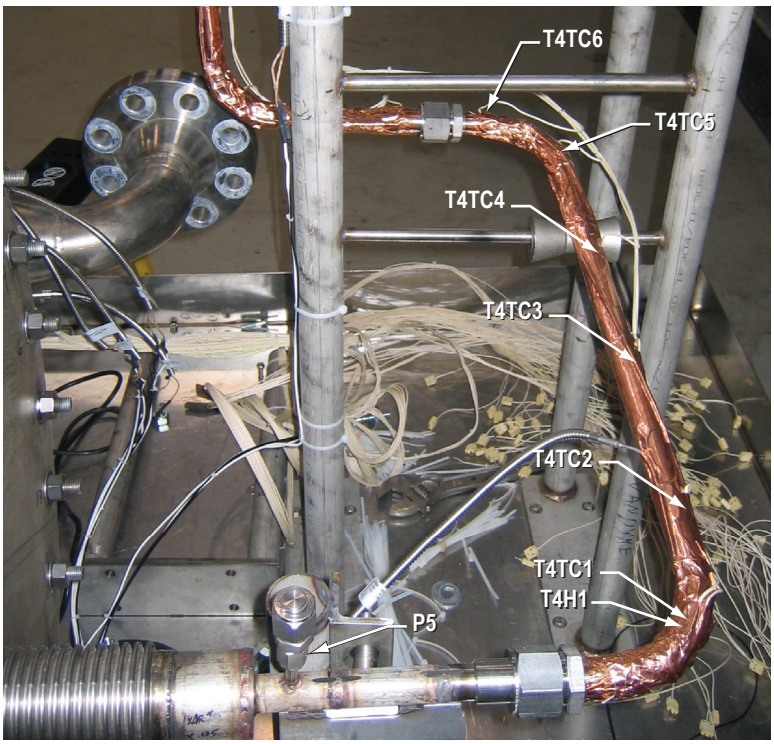

Figure 36. Photograph of T4.

4.11.5 Tube 5

Tube 5 (T5) was instrumented with five TCs (T5TC1–T5TC5) that record the Li temperatures as it moves from T4 to the core, as shown in figure 37. A pressure measurement is made at P6. TCs T5HA and T5HB are located underneath heater T5H1. Only one heater, T5H1, spirals around the tube section.

Figure 37. Photograph of T5.

4.11.6 Tube 6

Tube 6 (T6) was instrumented with four TCs (T6TC1– T6TC4) that record the Li temperatures as it moves to and from the LR into the system, as shown in figure 38. A hand-operated valve- (HOV-) V4 was to be converted to an ROV as discussed in section 4.9. Only one heater, T6H1, spirals around the tube section.

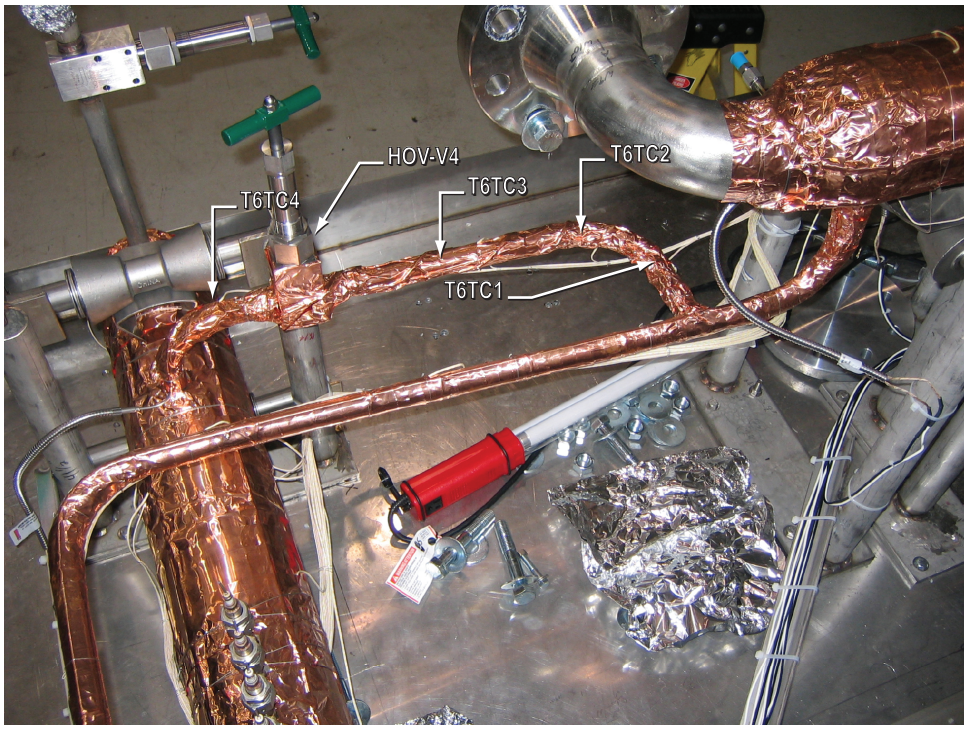

Figure 38. Photograph of T6.

5. MODELING AND TESTING

Initial experiments were performed to gain experience with handling Li in both solid and liquid form at elevated temperatures in order to understand the behavior of void formation in Li and to gather data that could be used to calibrate upgrades to a generalized fluid system simulation program (GFSSP) model. These upgrades would enable GFSSP to model the freeze/thaw of Li in the system to ultimately and hopefully produce a model that could be used to predict the freeze/thaw of a complete system. This ability would then aid in further designs of liquid Li systems.

5.1 Generalized Fluid System Simulation Program

The Li circuit was modeled using GFSSP. This is a general-purpose computer program for analyzing steady-state and time-dependent flow rates, pressures, temperatures, and concentrations in a complex flow network. The program is capable of modeling phase changes, compressibility, mixture thermodynamics, and external body forces such as gravity and centrifugal forces.

The program contains subroutines for computing 'real fluid' thermodynamic and thermophysical properties for 12 fluids. The program also provides the option for using any incompressible fluid with constant density and viscosity.

Seventeen different resistance/source options are provided for modeling momentum sources or sinks in the branches. These options include: (1) pipe flow, (2) flowthrough restriction, (3) noncircular duct, (4) pipe flow with entrance and/or exit losses, (5) thin, sharp orifice, (6) thick orifice, (7) square edge reduction, (8) square edge expansion, (9) rotating annular duct, (10) rotating radial duct, (11) labyrinth seal, (12) parallel plates, (13) common fittings and valves, (14) pump characteristics, (15) pump power, (16) valve with a given loss coefficient, and (17) a Joule-Thompson device.

GFSSP employs a finite volume formation of mass, momentum, and energy conservation equations in conjunction with the thermodynamic equations of state for real fluids. Mass, energy, and species conservation equations are solved at the nodes and the momentum conservation equations are solved in the branches. The system of equations describing the fluid network is solved by a hybrid numerical method that is a combination of the Newton-Raphson and successive substitution methods.

The computer program is composed of three major parts. The first part consists of the preprocessor subroutines that allow the user to interactively create the flow network model consisting of nodes and branches. All of the input specifications, including the boundary conditions, are specified through the preprocessor. The second major part of the program consists of the subroutines that provide the initial conditions and then develop and solve all of the conservation equations in the flow network. The third part of the program consists of the thermodynamic property programs that provide the necessary thermodynamic and thermophysical property data to solve the resulting system of equations.

The specific objective of the Li circuit analysis using GFSSP was to calculate pressure and temperature distribution in a Li-cooled reactor system in order to assess the location and constraints of pressure transducers necessary for circuit instrumentation. The model includes the pump, reactor core, HX, He line, and feed lines. The model calculates the pressure and temperature of each component during a steady-state operation. Figure 39 shows the GFSSP model graphical representation of the analysis.

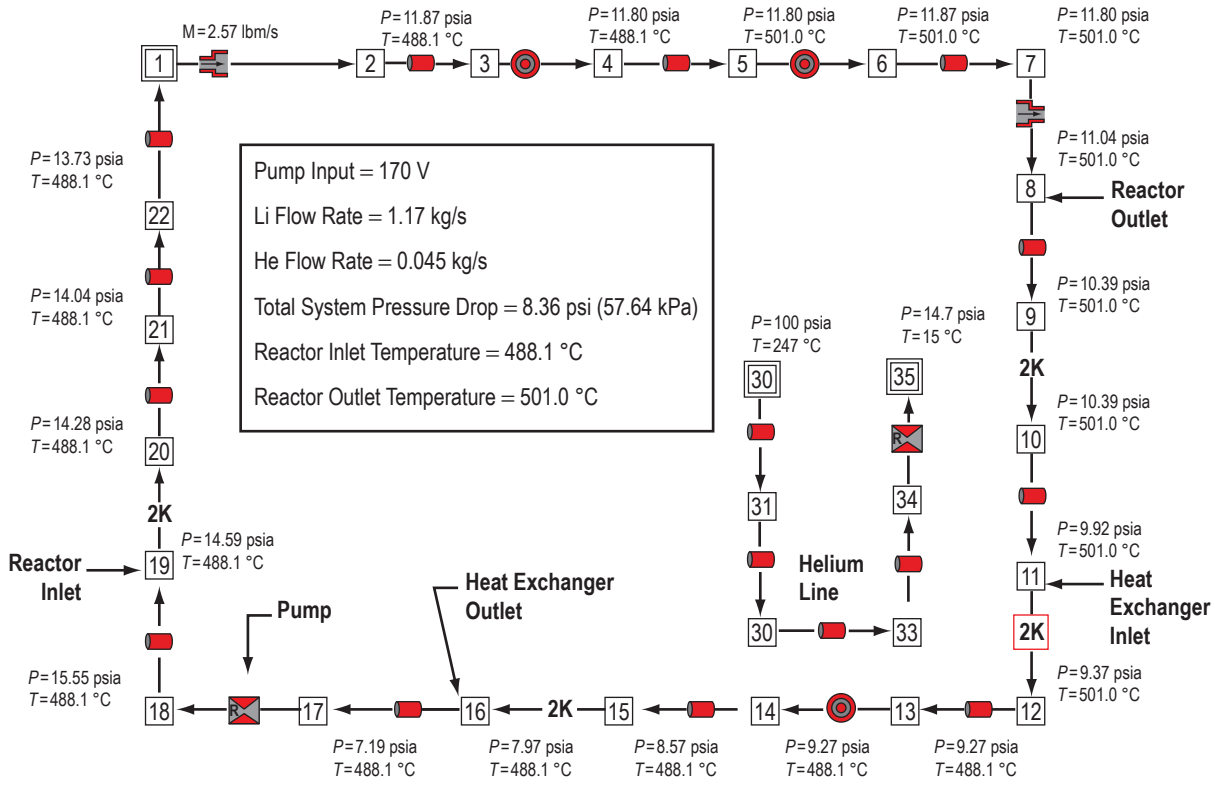

Figure 39. GFSSP model of the Li circuit.

The GFSSP analysis results provide numerical predictions of pressure and temperature at various locations in the flow circuit. Highlights of these results are:

- Electromagnetic pump is anticipated to raise the pressure from 49.64 kPa (7.2 psia) to 107.2 kPa (15.55 psia) at a flow rate of 1.17 kg/s (2.57 lb/s).
- Total pressure drop in the reactor is 24.48 kPa (3.55 psi).
- Total pressure drop in the HX is 13.44 kPa (1.95 psi).
- Total pressure drop in the feedline between the pump and reactor inlet is 6.62 kPa (0.96 psi).
- Total pressure drop in the feedline between the reactor outlet and HX inlet is 7.72 kPa (1.12 psi).

• Total pressure drop in the feedline between the HX outlet and pump is 5.399 kPa (0.783 psi).

• Total pressure drop in the system is 57.64 kPa (8.36 psi), which is in balance with the pressure rise in the pump.

In the reactor, temperature rises from 488 °C (910 °F) to 501 °C (934 °F). Temperature drops by the same amount in the HX. This confirms that the model correctly accounts for the cyclic boundary condition.

The temperature level of the Li system was determined by He inlet temperature and He flow rate. In the present model, He inlet temperature and He flow rate were set to 277 °C (477 °F) and 0.045 kg/s (0.1 lb/s), respectively.

From this model, the expected system pressures were used to specify the pressure transducers as well as to provide locations for placement.

5.2 Lithium Melt/Wetting

One of the first tests conducted was to visually identify the approximate wetting temperature of Li. These tests, while basic, were intended to give experience in three areas: (1) General physical manipulation of Li, (2) visual indication of wetting, and (3) experience with handling of Li at elevated temperatures, ≈300 °C (572 °F).

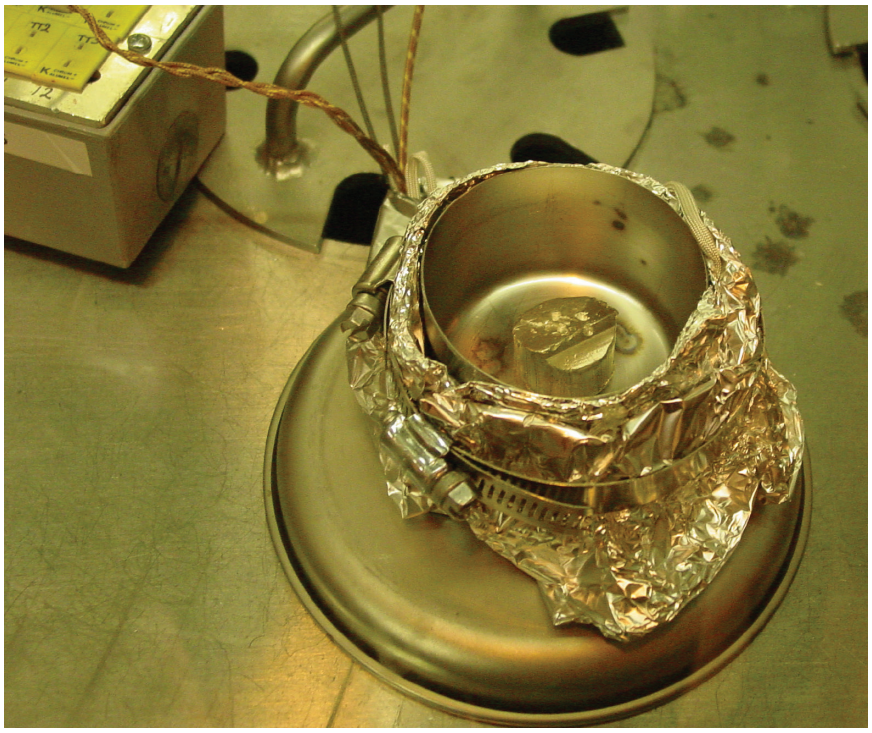

Figure 40. Stainless steel beaker with freshly sheared Li before melt.

A SS beaker was wrapped with heater tape and outfitted with TCs spot welded to the bottom surface (fig. 40). The beaker and the solid Li sample, packaged in foil wrap with Ar cover gas, were passed into a glove box. This glove box was designed to maintain an atmosphere having <1 ppm O_2, <1 ppm N_2, and <1 ppm water vapor, suitable for handling alkali metals such as Na, NaK, and Li. After trial and error, it was determined that the best method to cut the 1.27-cm- (0.5-in-) diameter, 15.24-cm- (6-in-) long piece of solid Li was using pruning shears. Sawing with a hacksaw quickly proved ineffective due to the gummy nature of the Li. A small piece was sheared off and placed in the beaker with three TCs that were connected to a data acquisition system programmed in LabVIEW. The beaker heater was turned on and the wetting temperature of the Li was observed. A cleaned but unbaked SS beaker in an Ar atmosphere (as opposed to actual conditions of a vacuum baking and vacuum loading) was considered a good condition in which to establish the upper limit wet temperature when combined with 98% pure Li (as opposed to the more pure 99.7% purchased for the circuit). The observed wetting temperature was 300 to 310 °C (572 to 590 °F).

5.3 Lithium Fill

Prior to filling the entire Li circuit with Li, a small test article was filled. This test article was used to gain further experience with Li and to gather data for the freeze/thaw tests; however, an equal amount of experience and information was gained from the fill process. Figure 41 shows the fill apparatus in a horizontal orientation. The actual orientation was vertical to allow gravity to help the Li move into the test article. Not shown are the tape heaters wrapped around the test article, transfer valve, and melt pot.

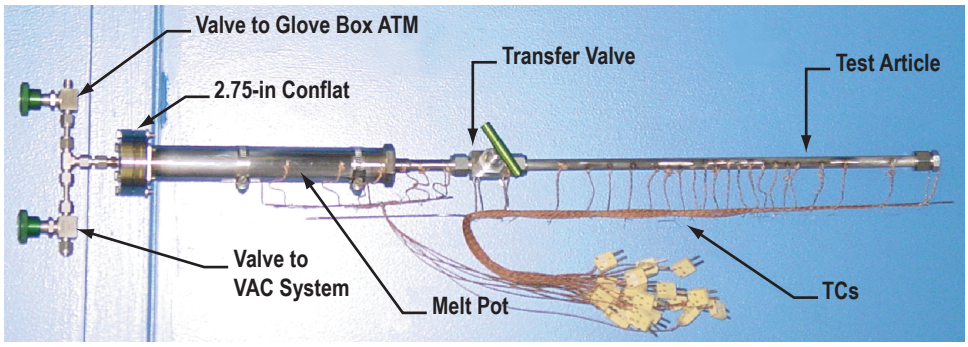

Figure 41. Lithium fill apparatus used to fill the test article.

To complete the test article fill, the melt pot was opened at the 6.99-cm (2.75-in) Conflat flanges. Pre-measured and weighed slugs of Li were placed in the melt pot. The entire vessel was baked out until the vacuum remained stable at 10^{-5} torr prior to introduction of the Li and again after the introduction of the Li. (The glove box atmosphere valve was closed and the vacuum valve was connected to a vacuum system with ion gauges.) Following melt pot bake-out, a vacuum was trapped in the test article by closing the transfer valve while under vacuum. The Li was melted to ≈300 °C (≈572 °F) under vacuum and the melt pot was gently tapped with a wrench until all of the gasses trapped in the melted Li evolved, as indicated on the ion gauges. The Li was introduced into the test article at 300 °C (572 °F) by isolating the vacuum system and opening the glove box atmosphere valve. When the transfer valve was opened, the transfer of the Li to the test article was assisted by the pressure difference (vacuum in the test article

and atmospheric pressure pushing on the Li in the melt pot) and gravity to overcome any surface tension or friction. This transfer was monitored and verified by recording TC data along the test article, the valve body, and the melt pot. The Li in the test article was then raised to 375 °C (707 °F) and the transfer valve was closed. When the Li cooled, a void was left in the test article and was used in follow-on testing in an attempt to understand void formation during freeze. Some of the most important lessons learned were:

- Solid Li outgasses when melted.
- TCs on the outside of the tubes normalize to the Li temperature.
- Wetting can be accomplished (as predicted) at the test temperatures.
- The technique for introducing Li was verified.

These lessons learned were applied to the design and operation of the circuit.

5.4 Lithium Freeze/Thaw Tests

Freeze and thaw tests were performed to provide hands-on experience: (1) With a freeze/thaw front and power heat loss values from the test section (article) to the environment, (2) to investigate void formation, and (3) to provide actual data for comparison to GFFSP module results. These tests were conducted in a vacuum chamber using a cable heater to supply heat to the valve end of the test article (fig. 42).

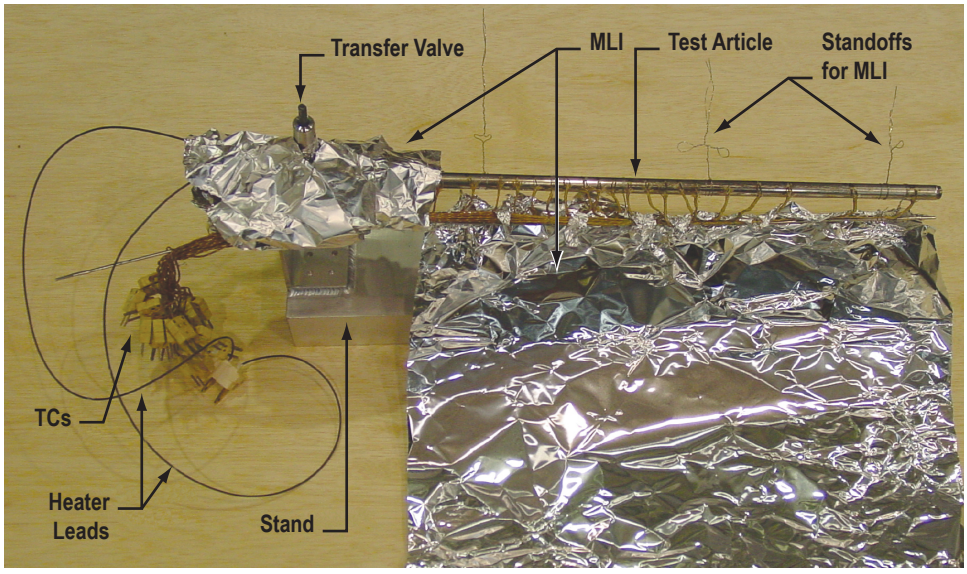

Figure 42. Freeze/thaw test article.

The test article was mounted on a stand at the valve end with the heat load applied at the other end via a cable heater. MLI consisting of loose wraps of aluminum foil was wrapped around the test article. (The test section is shown unwrapped in fig. 42.) The TCs were located at measured distances and used to gather the temperature data (fig. 43).

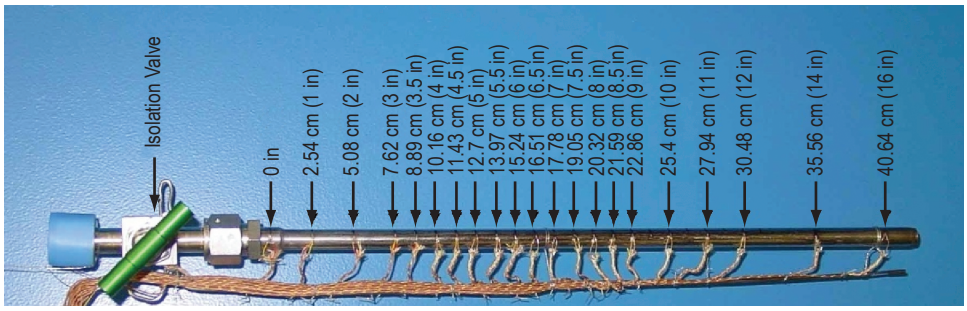

Figure 43. Freeze/thaw test article with TC locations at various distances.

Figure 44 shows a graph of data from a thaw cycle, and figure 45 shows data from a freeze cycle.

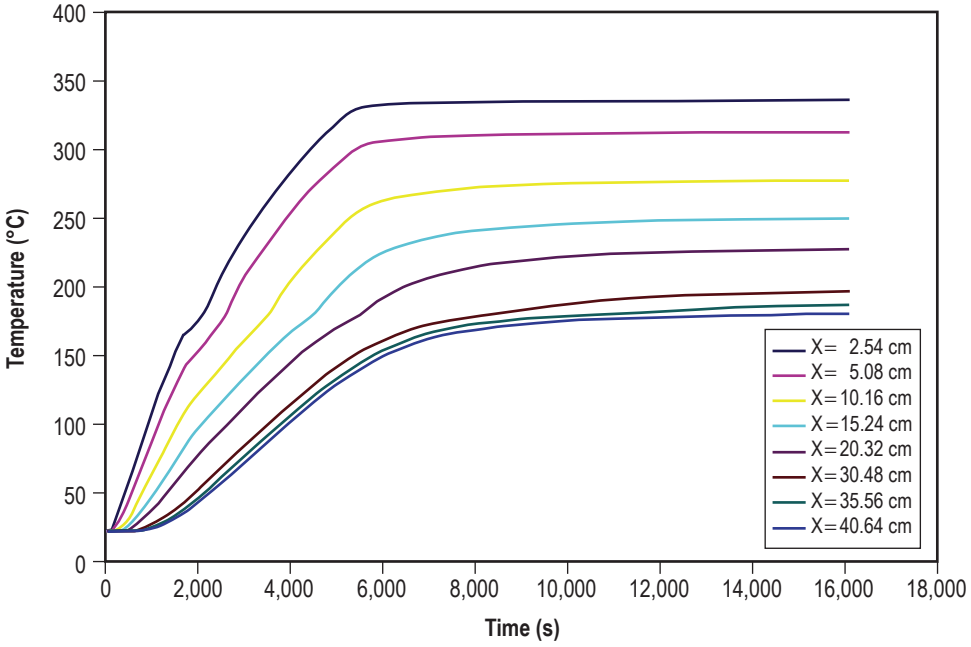

Figure 44. Measured temperature history during Li thawing.

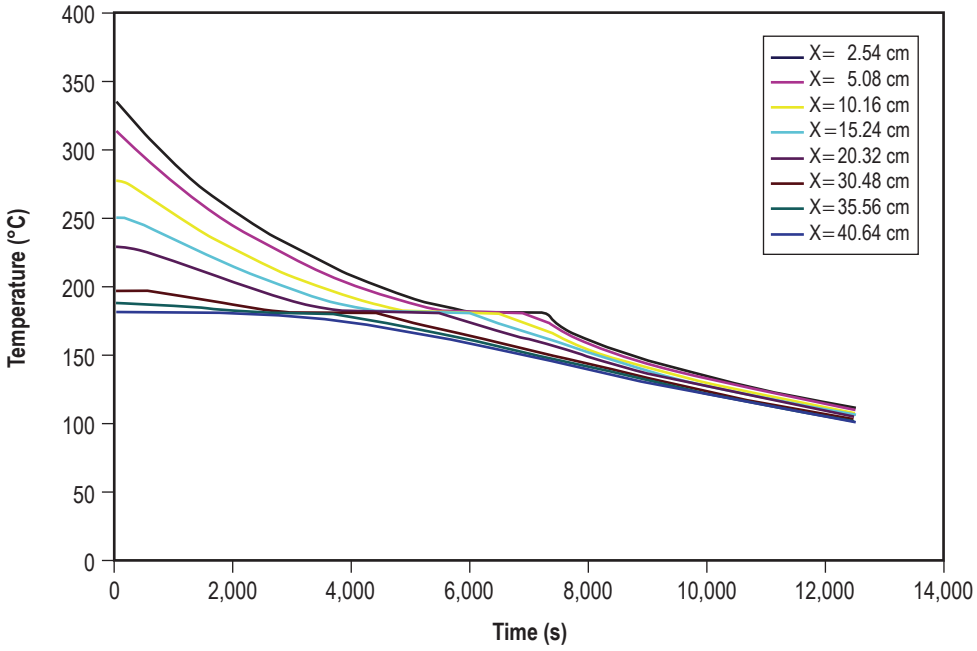

Figure 45. Measured temperature history during Li freezing.

5.5 Lithium Freeze/Thaw Modeling

Actual data taken during freeze/thaw testing were used to help develop and to calibrate a freeze/thaw node in GFSSP. The conjugate heat transfer option in GFSSP allows for modeling of heat conduction in static solid nodes that may be connected to fluid nodes. For this case, the modeling capability of heat conduction through solid nodes was upgraded to model phase change (thaw and freeze). Further details are provided in reference 6.

5.5.1 Lithium Thaw Model

The measured temperature history at eight axial locations during Li thaw is shown in figure 44. The temperature history shows a point of inflection at the melting temperature. This is due to the change in thermophysical properties between solid and liquid Li. After 10,000 s, the temperature distribution began to exhibit steady-state behavior. The point of inflection is, therefore, less prominent at locations close to the free end of the rod.

The predicted temperature history for the same locations is shown in figure 46. Similar behavior is present in the predicted temperature history in which a point of inflection is observed at the melting temperature and steady-state characteristics are shown after 10,000 s. The slightly unsteady temperature history observed near the melting point can be attributed to the discontinuity in thermophysical properties during the phase change.

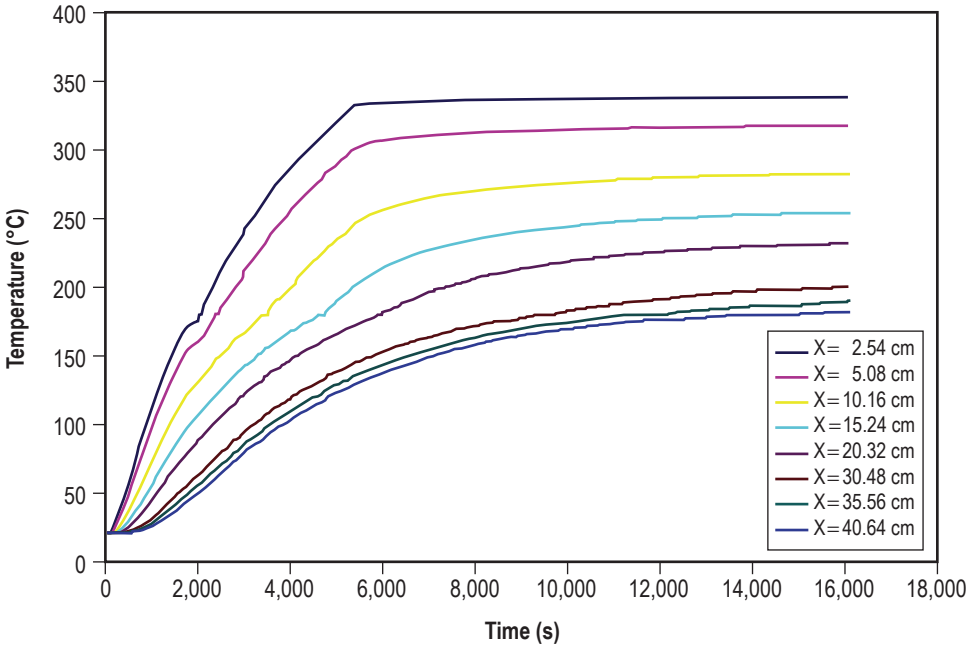

Figure 46. Predicted temperature history of Li thawing.

Overall, good correlation was observed between prediction and measurement. A discrepancy, however, is observed near the free end of the rod. This discrepancy may be attributed to approximations made in calculating the heat loss to the wall and through the support structure.

5.5.2 Lithium Freeze Model

The freeze model used the same nodal structure as the thaw model. However, the initial and boundary conditions were different. After 16,116 s, the heater was turned off and the test assembly was allowed to cool. The temperature measured at that instant was assigned to all 19 GFSSP nodes.

Figure 45 shows the measured temperature history during Li freeze at the locations where thaw results were shown previously. Unlike during the thaw cycle, the freeze line propagates from the free end to the valve end. It took a little over 7,000 s to freeze the entire rod. The predicted temperature history is shown in figure 47. The predicted behavior of the freezing process resembles the pattern observed in the test.

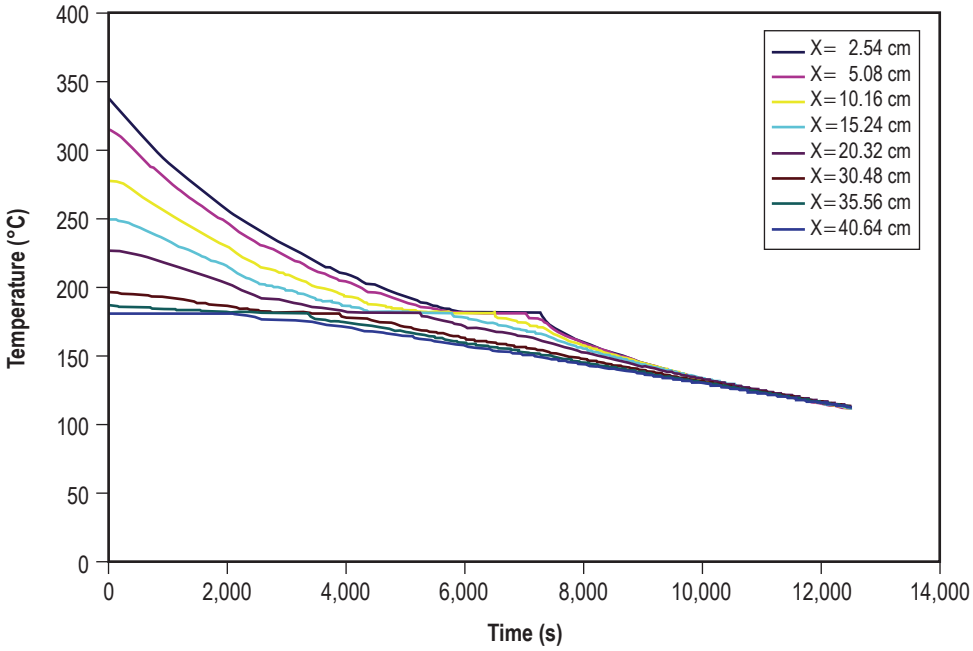

Figure 47. Predicted temperature history of Li freezing.

As with the thaw model, there is a good agreement between predictions and measurements. The fact that temperature history during thaw is very different from the freeze process is predicted accurately by the numerical model. The observed disagreement near the free end is due to approximation in the heat loss calculation.

Modeling of Li phase change due to heat conduction was done using GFSSP. It shows that the numerical predictions compare well with test data for both thaw and freeze processes.

6. CONCLUSIONS

The SS, Li circuit test section design project was cancelled due to a shift in program direction with the selection of a gas-cooled reactor concept to support proposed nuclear electric propulsion. As a result, all activities have been closed out using the most logical approach to terminate procurements in an effort to recoup cost without total loss. The circuit was removed from the vacuum test chamber and has been dressed for storage. This Technical Publication has summarized the design of the pumped liquid metal Li flow circuit as of May 1, 2005.

REFERENCES

1. Rhys, N.O., Ph.D.: "A Brief Review of Thermophysical Properties of Lithium," NASA Marshall Space Flight Center Internal Document, ER11-04-WI4A-002-1, February 11, 2005.

2. Chopra, O.K.; and Smith, D.L.: "Corrosion of Ferrous Alloys in a Flowing Lithium Environment," *J. Nucl. Mater.*, Vols. 133–134, pp. 861–866, August 1985.

3. Tortorelli, P.F.; and Chopra, O.K.: "Corrosion and Compatibility Considerations of Liquid Metals for Fusion Reactor Applications," *J. Nucl. Mater.*, Vol. 103, pp. 621–632, 1981.

4. Poston, D.; Kapernak, R.; Willcutt, G.; and Guffee, R.: "100 kWt SS NaK Cooled Reactor Concept," Los Alamos National Laboratory Design Study Presentation, Los Alamos, NM, 2003.

5. Bragg-Sitton, S.M.: "High Purity Lithium Suppliers in the United States," ER11-04-WI4A-005, NASA Marshall Space Flight Center, AL, October 12, 2004.

6. Majumdar, A.K.: "Verification of Numerical Modeling of Lithium Thaw and Freeze," ER11-04-WI4A-008, NASA Marshall Space Flight Center, AL, March 8, 2005.

REPORT DOCUMENTATION PAGE

Form Approved
OMB No. 0704-0188

1. REPORT DATE *(DD-MM-YYYY)*	2. REPORT TYPE	3. DATES COVERED *(From - To)*
01–08–2010	Technical Publication	

4. TITLE AND SUBTITLE

Documentation of Stainless Steel Lithium Circuit Test Section Design

5a. CONTRACT NUMBER

5b. GRANT NUMBER

5c. PROGRAM ELEMENT NUMBER

6. AUTHOR(S)

T.J. Godfroy* and J.J. Martin
with Supplemental Information by E.T. Stewart and N.O. Rhys**

5d. PROJECT NUMBER

5e. TASK NUMBER

5f. WORK UNIT NUMBER

7. PERFORMING ORGANIZATION NAME(S) AND ADDRESS(ES)

George C. Marshall Space Flight Center
Marshall Space Flight Center, AL 35812

8. PERFORMING ORGANIZATION REPORT NUMBER

M–1286

9. SPONSORING/MONITORING AGENCY NAME(S) AND ADDRESS(ES)

National Aeronautics and Space Administration
Washington, DC 20546–0001

10. SPONSORING/MONITOR'S ACRONYM(S)

NASA

11. SPONSORING/MONITORING REPORT NUMBER

NASA/TP—2010–216437

12. DISTRIBUTION/AVAILABILITY STATEMENT

Unclassified-Unlimited
Subject Category 29
Availability: NASA CASI (443–757–5802)

13. SUPPLEMENTARY NOTES

Prepared by the Propulsion Systems Department, Engineering Directorate
* Maximum Technology Corporation, Huntsville, AL 35816
** Yetispace, Inc., Huntsville, AL 35802

14. ABSTRACT

The Early Flight Fission–Test Facilities (EFF–TF) team was tasked by Naval Reactors Prime Contract Team (NRPCT) to design, fabricate, and test an actively pumped lithium (Li) flow circuit. This Li circuit takes advantage of work in progress at the EFF–TF on a stainless steel sodium/potassium (NaK) circuit. The effort involved modifying the original stainless steel NaK circuit such that it could be operated with Li in place of NaK. This new design considered freeze/thaw issues and required the addition of an expansion tank and expansion/extrusion volumes in the circuit plumbing. Instrumentation has been specified for Li and circuit heaters have been placed throughout the design to ensure adequate operational temperatures and no uncontrolled freezing of the Li. All major components have been designed and fabricated prior to circuit redesign for Li and were not modified. Basic circuit components include: reactor segment, Li to gas heat exchanger, electromagnetic liquid metal pump, load/drain reservoir, expansion reservoir, instrumentation, and trace heaters. The reactor segment, based on a Los Alamos National Laboratory 100-kW design study with 120 fuel pins, is the only prototypic component in the circuit. However, due to earlier funding constraints, a 37-pin partial-array of the core, including the central three rings of fuel pins (pin and flow path dimensions are the same as those in the full design), was selected for fabrication and test. This Technical Publication summarizes the design and integration of the pumped liquid metal Li flow circuit as of May 1, 2005.

15. SUBJECT TERMS

space reactor, alkali metal, liquid metal, lithium circuit, pumped loop

16. SECURITY CLASSIFICATION OF:			17. LIMITATION OF ABSTRACT	18. NUMBER OF PAGES	19a. NAME OF RESPONSIBLE PERSON
a. REPORT	b. ABSTRACT	c. THIS PAGE			STI Help Desk at email: help@sti.nasa.gov
U	U	U	UU	60	19b. TELEPHONE NUMBER *(Include area code)*
					STI Help Desk at: 443–757–5802

National Aeronautics and
Space Administration
IS20
George C. Marshall Space Flight Center
Marshall Space Flight Center, Alabama
35812